NAVAL POSTGRADUATE SCHOOL
Monterey, California

THESIS

TWO-DIMENSIONAL MODELING OF ALUMINUM GALLIUM NITRIDE/GALLIUM NITRIDE HIGH ELECTRON MOBILITY TRANSISTOR

by

Kenneth L. Holmes

June 2002

Thesis Advisor:	Todd R. Weatherford
Second Reader:	Ronald Pieper

THIS PAGE INTENTIONALLY LEFT BLANK

REPORT DOCUMENTATION PAGE			Form Approved OMB No. 0704-0188
Public reporting burden for this collection of information is estimated to average 1 hour per response, including the time for reviewing instruction, searching existing data sources, gathering and maintaining the data needed, and completing and reviewing the collection of information. Send comments regarding this burden estimate or any other aspect of this collection of information, including suggestions for reducing this burden, to Washington headquarters Services, Directorate for Information Operations and Reports, 1215 Jefferson Davis Highway, Suite 1204, Arlington, VA 22202-4302, and to the Office of Management and Budget, Paperwork Reduction Project (0704-0188) Washington DC 20503.			
1. AGENCY USE ONLY *(Leave blank)*	**2. REPORT DATE** June 2002	**3. REPORT TYPE AND DATES COVERED** Master's Thesis	
4. TITLE AND SUBTITLE: Title (Mix case letters) Two-Dimensional Modeling of Aluminum Gallium Nitride/Gallium Nitride High Electron Mobility Transistor			**5. FUNDING NUMBERS**
6. AUTHOR(S) Holmes, Kenneth L.			
7. PERFORMING ORGANIZATION NAME(S) AND ADDRESS(ES) Naval Postgraduate School Monterey, CA 93943-5000			**8. PERFORMING ORGANIZATION REPORT NUMBER**
9. SPONSORING / MONITORING AGENCY NAME(S) AND ADDRESS(ES) N/A			**10. SPONSORING / MONITORING AGENCY REPORT NUMBER**
11. SUPPLEMENTARY NOTES The views expressed in this thesis are those of the author and do not reflect the official policy or position of the Department of Defense or the U.S. Government.			
12a. DISTRIBUTION / AVAILABILITY STATEMENT Approved for public release; distribution is unlimited			**12b. DISTRIBUTION CODE** A

13. ABSTRACT ***(maximum 200 words)***

Gallium Nitride (GaN) High Electron Mobility Transistors (HEMT's) are microwave power devices that have the performance characteristics to improve the capabilities of current and future Navy radar and communication systems. The Office of Naval Research (ONR) is funding research for the development of GaN-based microwave power amplifiers for use in future radar and communication systems. This thesis studies the effects of AlGaN/GaN HEMTs' polarization, piezoelectric (PZ) and spontaneous, properties utilizing the commercially available Silvaco Atlas™ software for modeling and simulation. The polarization properties are suspected to enhance the two-dimensional electron gas (2DEG) at the AlGaN/GaN interface.

14. SUBJECT TERMS Gallium Nitride, High Electron Mobility Transistor, Piezoelectric effect			**15. NUMBER OF PAGES** 79
			16. PRICE CODE
17. SECURITY CLASSIFICATION OF REPORT Unclassified	**18. SECURITY CLASSIFICATION OF THIS PAGE** Unclassified	**19. SECURITY CLASSIFICATION OF ABSTRACT** Unclassified	**20. LIMITATION OF ABSTRACT** UL

NSN 7540-01-280-5500 Standard Form 298 (Rev. 2-89)
Prescribed by ANSI Std. 239-18

THIS PAGE INTENTIONALLY LEFT BLANK

Approved for public release; distribution is unlimited

TWO-DIMENSIONAL MODELING OF ALUMINUM GALLIUM NITRIDE/GALLIUM NITRIDE HIGH ELECTRON MOBILITY TRANSISTOR

Kenneth L. Holmes
Lieutenant, United States Navy
B.S., Prairie View Agriculture & Mechanical University, 1993

Submitted in partial fulfillment of the
requirements for the degree of

MASTER OF SCIENCE IN ELECTRICAL ENGINEERING

from the

NAVAL POSTGRADUATE SCHOOL
June 2002

Author: Kenneth L. Holmes

Approved by: Todd Weatherford
Thesis Advisor

Ronald Pieper
Second Reader

Jeffrey B. Knorr
Chairman, Department of
Electrical and Computer Engineering

THIS PAGE INTENTIONALLY LEFT BLANK

ABSTRACT

Gallium Nitride (GaN) High Electron Mobility Transistors (HEMT's) are microwave power devices that have the performance characteristics to improve the capabilities of current and future Navy radar and communication systems. The Office of Naval Research (ONR) is funding research for the development of GaN-based microwave power amplifiers for use in future radar and communication systems. This thesis studies the effects of AlGaN/GaN HEMTs' polarization, piezoelectric (PZ) and spontaneous, properties utilizing the commercially available Silvaco Atlas™ software for modeling and simulation. The polarization properties are suspected to enhance the two-dimensional electron gas (2DEG) at the AlGaN/GaN interface.

THIS PAGE INTENTIONALLY LEFT BLANK

TABLE OF CONTENTS

THIS PAGE INTENTIONALLY LEFT BLANK

LIST OF FIGURES

LIST OF TABLES

THIS PAGE INTENTIONALLY LEFT BLANK

ACKNOWLEDGMENTS

I sincerely thank the following individuals who made it possible for me to complete this thesis: Prof. Weatherford for providing clear guidance, keeping the project on track, and ensuring the quality of the final product. Dr. Umesh Mishra for kindly assisting with the background content for GaN modeling. LT Karl Eimers, Dr. Steve Binari, Dr. Mario Ancona, Dr. Weber, Dr. Specht, and Dr. Feick for beginning this valuable work. My parents, Ossie and Jewell Henry, for their love and devotion in raising me. My wife, Myeshea, and my son, Devin, for being a constant reminder of why we defend our country. My brothers- and sisters-in-Christ for being closer to me than most of my own family. My Pastor, Reverend Anthony D. Dunham, for supporting me and advising me through the *good days* and *bad days*. Most of all, I thank my Heavenly Father, whom, without Him, nothing is possible but, with Him, nothing is impossible. And, I thank His only begotten son, Jesus Christ, who is God and who sacrificed his life so that I may have everlasting life.

EXECUTIVE SUMMARY

A computer model of Aluminum Gallium Nitride (AlGaN)/Gallium Nitride (GaN) High Electron Mobility Transistors (HEMTs) has been developed for the purpose of designing and modifying high power and high frequency power amplifiers. GaN-based HEMT power amplifiers are being investigated for application in future military radar and communication systems. This model includes the impact of the AlGaN/GaN polarization, piezoelectric and spontaneous, effects based upon the material parameters of AlGaN, GaN, and HEMTs.

The polarization effects result from the GaN's noncentrosymmetric crystal structure combined with strain induced at the AlGaN/GaN heterojunction due to their lattice mismatch. This effect results in a large electron concentration at the heterojunction thus providing exceptional conductivity of electron current. As a material, GaN has a large energy bandgap, high breakdown voltage, and high peak electron velocity. The HEMT's characteristic heterojunction produces a quantum well which further enhances the speed of electron transport from source to drain contacts and reduces electron scattering.

The Silvaco software, a physics-based modeling program, was utilized to model and simulate an $Al_{0.3}Ga_{0.7}N$/GaN HEMT. The physical characteristics of an AlGaN layer grown on top of a GaN layer causes the production of dipoles in both layers. The software modifications use that concept.

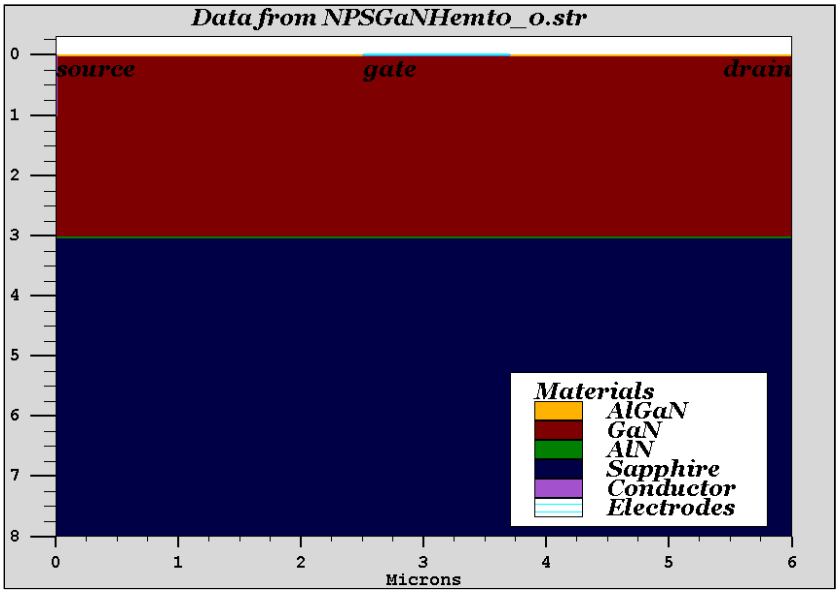

Figure a. ATLAS-generated representation of AlGaN/GaN HEMT

Simulations were run on a model based on an actual device tested at the Naval Research Laboratory (NRL). The model proved capable of matching the expected energy band profile and electron concentration near the heterojunction.

The model with a matching Al mole fraction (x = 0.3) was run through gate biasing conditions and compared with measured results provided by NRL and simulated previously by the Naval Postgraduate School. The device was simulated under matching gate biases and drain voltage ramping. The resultant IV curves displayed an above-average correspondence between modeled and measured results. Numerous combinations of electron mobility, velocity saturation, and gate work functions were attempted to improve IV curve correlation. The reported results were derived from a simulation run of the reported modeling program. Possible methods for improving model accuracy are discussed and recommended for future research and study.

THIS PAGE INTENTIONALLY LEFT BLANK

I. INTRODUCTION

A. BACKGROUND

The advancement of radar and communication technology is both vital and necessary for the continued accomplishment of the Navy's mission to: (1) protect friendly naval forces; (2) project national power; and (3) protect national interests. One of the key components is the further development of radio frequency (RF) amplifiers. Normally, RF waves are formed by relatively small and physically fragile electronics and, as a result, RF amplifiers are used to magnify the respective waves prior to transmission. Many systems, such as the Aegis Weapons Systems, use travelling-wave vacuum tube (TWT) technology to perform the RF amplification. Unfortunately, TWT's have continually demonstrated a high level of performance degradation in respect to service time and a high cost.

Solid-state technology, namely, semiconductor amplifiers, offers the most promising alternative to TWT amplifiers. Incorporating a smaller size coupled with higher reliability, semiconductor amplifiers offer a greater ease of manufacturing, packaging, and handling than the TWT's. Although, semiconductor amplifiers cannot currently match the maximum amplification of TWTs, they demonstrate respectable power levels with lower distortion levels than TWT's, especially over extended periods of time [1], [2].

Field Effect Transistors (FET's) and, specifically, High Electron Mobility Transistors (HEMT's) are excellent RF power amplifiers especially above 4 GHz and where low noise is vital. Due to environmental and man-made conditions, low noise is essential for radar systems' optimal performance. Although, HEMT's are relatively new, in relation to FET's, they have demonstrated great potential as high-speed power amplifiers. In general, FET's have displayed superior power gains, lower noise, and higher output power capabilities than their historic competitor, the bipolar junction transistor (BJT) [3]. However, the HEMT, has demonstrated the highest current-gain cutoff frequency of any current semiconductor device at 472 GHz [4].

As a compound semiconductor, Gallium Nitride (GaN) has the potential to be the leader in RF amplification because of its high frequency and high temperature capabilities and extremely high power output [1]. According to the Office of Naval Research, GaN amplifiers will take the place of vacuum tubes in most Navy radar systems once they are available. Because GaN can deliver up to ten times more power at microwave frequencies than current Silicon (Si) or Gallium Arsenide (GaAs) semiconductors used in some radar systems, it is expected to deliver large improvements in performance.

Computer software modeling has proven to be a versatile and valuable tool for engineering design and analysis. Recently, the Silvaco software applications have come to the forefront of engineering design and analysis of semiconductor devices and processes. In lieu of this, GaN-based devices require special attention and consideration for computer modeling and simulation due to their inherent polarization, piezoelectric (PZ) and spontaneous, properties. Considerable research time and funding has been devoted toward these and other nitride-based devices, and has included the establishment of select constants for their PZ properties and related effects. The polarization effects of GaN-based semiconductor devices have not been accurately modeled in a Technology Computer Aided Design (TCAD) program.

The GaN's PZ effect is its physical property to exhibit polarization when strained. This polarization results in lowered resistivity due to the presence of extra charge carriers thus greater current flow and power. Adding mechanical strain to a device might further enhance PZ effect [1].

B. RELATED WORK

The Naval Research Laboratory (NRL) and ONR continue to fund research through educational institutions and industry on GaN HEMT power amplifiers. NRL is modeling devices of their own construction [5]. NRL's models do not automatically account for the piezoelectric effect. The intent of this work is to aid their efforts and take a further step in accurately replicating the AlGaN/GaN HEMT.

The University of California at Santa Barbara is computer modeling AlGaN/GaN HEMT's based upon the field plate technique and surface donor-like traps and is focused on breakdown voltage research [6]. Their models do not automatically account for the piezoelectric effect, either. This work can aid in developing closer correlation between computer modeling and experimental data.

The Naval Postgraduate School has modeled AlGaN/GaN HEMT's using the Silvaco Software. That work focused upon modeling an existing HEMT's using Silvaco's C-INTERPRETER [1]. This work will aid in refining the previous modeling by establishing a base Silvaco code, using a dipole technique, to compare against experimental data and previous modeling.

C. OBJECTIVES

This work seeks to increase the Navy's capability to computer model GaN HEMT's by providing working Silvaco Software models of an existing GaN HEMT device. The models developed are distinguished in that they incorporate the piezoelectric effect using accepted constants, a dipole-concept approach, and computer program generated values.

THIS PAGE INTENTIONALLY LEFT BLANK

II. TRANSISTOR FUNDAMENTALS

A. FIELD EFFECT TRANSISTOR

FET's were the first solid-state transistors, or transfer resistors. Since their creation in the 1950's, FET's have distinguished themselves from other transistors through their ease of production and compact nature. Thanks to the computer industry, the FET (specifically the MOSFET) is currently the most produced manmade object in the world [1][7].

As noted by the name, FET's operate based upon the field effect phenomenon. The basic FET requires three contacts and a semiconductor material. The three contacts, source, gate, and drain, perform functions to facilitate the flow of electrons and current. The source, an ohmic contact, is the electrons' entry point to the transistor from the external circuit. The drain, an ohmic contact, is the electrons' exit point from the transistor to the external circuit. The gate, a rectifying contact, is the "electron flow" controller. The gate controls electron flow by modulating the conductance/resistance of the semiconductor material by applying a voltage to the semiconductor and thereby modulates the current flow through the FET (Figure 1). Electric current entering/leaving the FET is allowed to flow freely, restricted, or not at all depending on the voltage applied at the gate.

The gate to drain voltage difference will cause a depletion region (or an inversion layer) to grow in the vicinity of the gate. When the gate is oppositely biased from the source-drain voltage difference, the depletion region will grow until it "pinches off" current flow. As a result of pinch off, the amount of current flowing from source to drain is limited to its existing level. The device will shut off when no source-drain voltage difference exists and the gate is biased enough to create a complete depletion region. The transistor works because the gate's voltage controls the size of the depletion region present in the semiconductor.

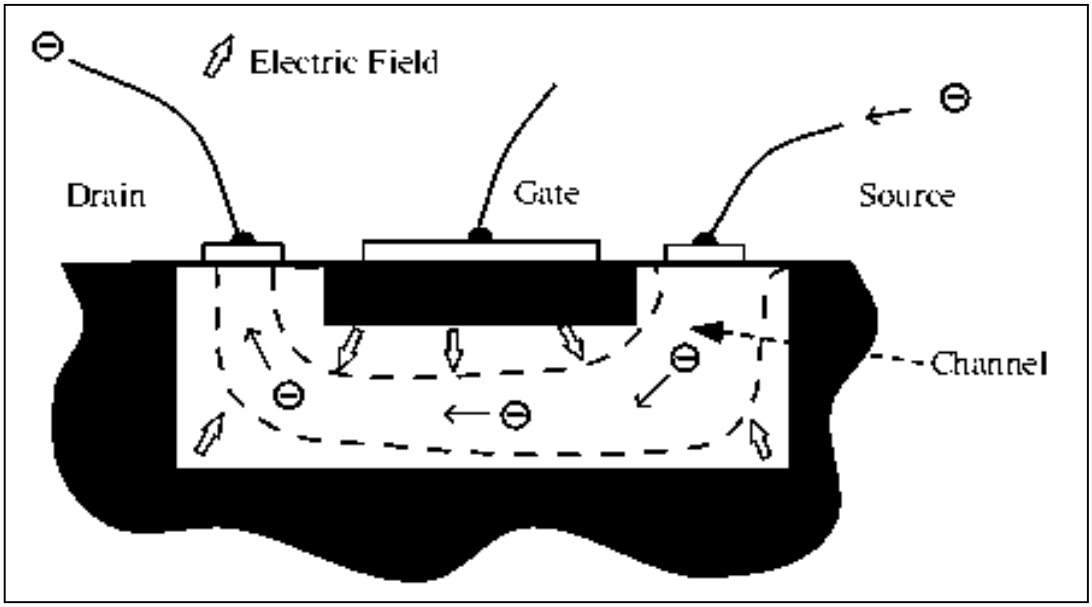

Figure 1. Basic FET Operation.

B. HIGH ELECTRON MOBILITY TRANSISTOR

The HEMT has gone by several different names: modulation-doped field-effect transistor (MODFET); heterostructure field-effect transistor (HFET); and selectively doped heterojunction transistor (SDHT). Regardless of the name used, these devices have unique performance characteristics that make them very attractive for military and civilian wireless communications and military radar applications. These characteristics are directly related to the type of carrier channel developed at the transistors' heterojunction. The carrier channel, a quantum well with a two-dimensional electron gas (2DEG), allows electrons to flow in only two dimensions vice three.

The 2DEG is formed at the heterojunction as a result of the conduction band offset (ΔE_C) between the two materials. At the interface, the material with the narrower bandgap will have its conduction band pulled down to the fermi level which will make the junction highly conductive. This material's conduction band rises with depth relative to the heterojunction and guides electrons toward the material interface. On the other side of the junction, the conduction band is much higher and prevents electrons from

traveling past the material interface (Figures 2 & 3). As a result, a quantum well is produced.

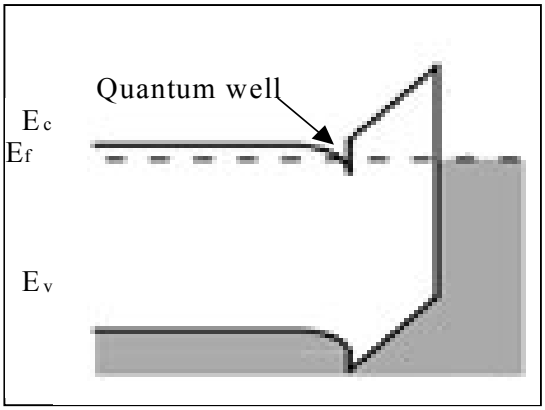

Figure 2. Two-dimensional HEMT energy band diagram with electric field applied.

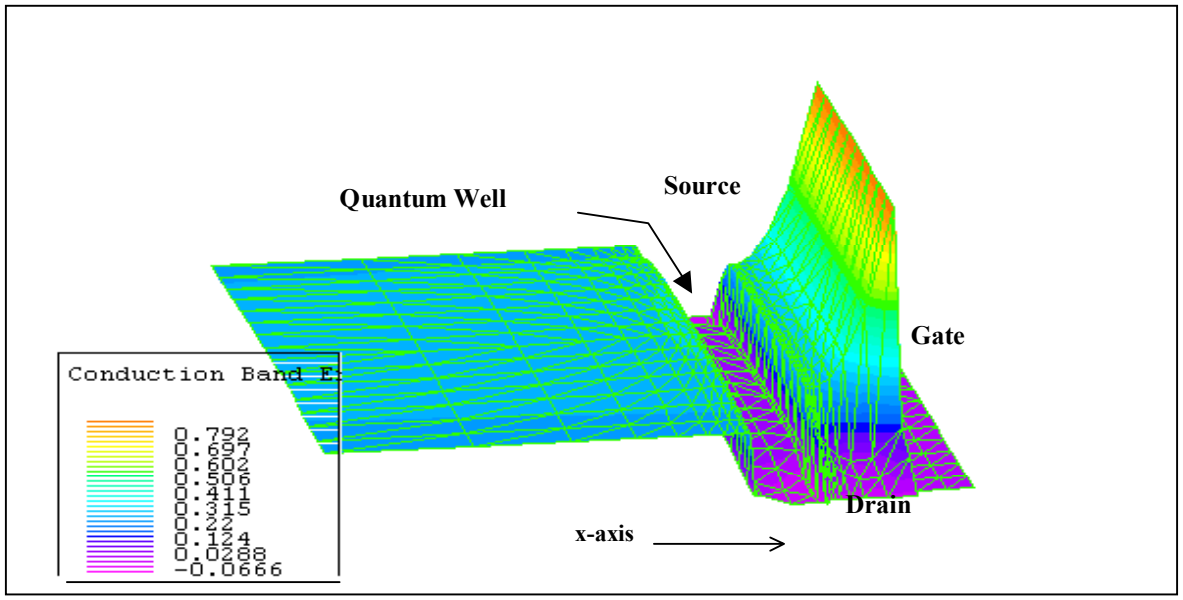

Figure 3. Three-dimensional energy (conduction) band diagram for unbiased HEMT.

In the quantum well, no electron can be placed at energies lower than the energy level that corresponds to the half-wavelength of the electron [8]. This energy level is called the first energy subband and is below the fermi level (E_f). The second energy subband corresponds to the electron's full-wavelength and is above E_f. Due to the slope

and height of the conduction bands relative to E_f and the first energy subband, electrons can not move freely or randomly scatter in the direction of the quantum well's cross section (x-axis). In Figure 3, observation of the first energy subband would suggest approximately zero electron movement in the x-direction but considerable movement in the y and z directions (two-dimensions). Relating the motion of molecules in gases to the motion of electrons in a semiconductor crystal has fostered the "electron gas" concept. The combination of two-dimensional movement and the "electron gas" concept has resulted in these electrons being referred to as the 2DEG.

The advantages of the 2DEG are that there is reduced scattering in two-dimensional motion vice three, and this causes reduced noise levels and increased electron mobility. Both properties are very desirable in high frequency and low noise

	Si	GaAs	SiC	GaN
Bandgap (eV)	1.1	1.4	3.25	**3.4**
Tmax (^{0}C)	300	440	1250	**1310**
Thermal Conductivity (W/cm K @ RT)	1.5	0.5	3.5	**1.3**
Electron Mobility (cm 2/Vs @$N_D = 10^{16}$ cm^{-3}	1200	6500	500	**600**
Sat. Electron Velocity V_{sat} (in 10^7 cm/s)	1.0	0.8	2.0	**2.5**
Breakdown Field E_{br} (MV/cm)	0.3	0.4	3.0	**3.5**
Johnson's FOM $\mu E_{br}^2 V_{sat}^2$	1	7	400	**850**

Wide Bandgap

Thermal Properties Synergistic With High Power Advantage

Principal Weakness: Not Significant for Power Devices at High Voltages

Key Electrical Parameters for High Power Operation

Thermal Effects Usually Constrain Full Exploitation

Table 1. Semiconductor Properties.

applications such as, communications and radar. For some current applications, HEMTs have been constructed of non-Silicon semiconductors such as, GaAs and GaN, due to the specific material properties of these compound semiconductors (Table 1). Additionally, for AlGaN/GaN, 2DEG mobility was found to be $1.9x10^4$ cm^2/Vs @ 10K [9].

C. GALLIUM NITRIDE

Group III-nitride materials are ideal for high power and high temperature devices due to their large energy bandgap, high breakdown voltage, high peak electron velocity and high electron sheet density in channels when used in a heterostructure [1]. Nitride materials benefit from having large and direct bandgaps which makes them very capable and well suited to handle environmentally hostile conditions such as, those at high altitudes or in space, and very useful in optical applications. Although other materials such as, Silicon Carbide (SiC), have some similar properties, nitride materials can form better heterostructures and ohmic contacts, and appear to be more promising. Of the nitride materials, the GaN based devices have demonstrated the most functionality and garnered the most interest. Figure 4 is a depiction of a Wurtzite GaN molecule.

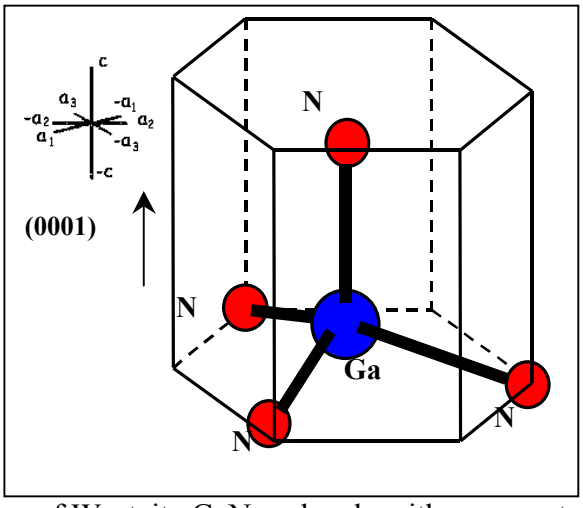

Figure 4. Depiction of Wurtzite GaN molecule with representative hexagonal axes

The GaN devices' major drawbacks are: (1) challenges in the manufacturing process that have lead to reliability problems and excessive costs; and (2) electron mobility is not significant for power devices at high voltages. Along with other Nitride materials, GaN has been difficult to chemical etch because of its characteristically inert nature. Because of their high melting temperatures and pressures, normal etching methods such as, the Czochralski method, have proven ineffective on Nitride materials. The commercial semiconductor industry, some educational institutions, and various research entities have performed significant research into the growth of quality GaN crystals to produce better performance and fewer defects, however, further work needs to be performed.

In general, high temperatures degrade electronic performance because electric-field mobility and electric-field electron velocities can be adversely affected by rising temperature. For the production of GaN devices, like all high power devices, the problem of thermal dissipation had to be addressed. This has made the search and selection of a suitable substrate of paramount importance.

In the past, Sapphire has been a successful substrate for GaN devices. Sapphire was the first successful substrate used with GaN by Shui Nakamura (who made a blue LED) at Nichia Chemical in Japan [10]. Silicon Carbide, however, can conduct heat at seven times the rate of Sapphire [11]. Thus, Silicon Carbide appears to be a better GaN substrate material than Sapphire. Individually, SiC is a useful wide bandgap semiconductor, as evidenced by its material properties in Table 1, and is much easier to fabricate than Sapphire. In addition to boasting a much better thermal conductivity and a greater ease of fabrication, SiC has a lower difference between lattice constants (3% difference for GaN/SiC compared to 13% for GaN/Sapphire) which reduces the molecular stress between semiconductor and substrate. Also, as a result of lower dislocation density, SiC produces a larger 2DEG electron concentration (~$1.4 \times 10^{13}/cm^2$ vice $1 \times 10^{13}/cm^2$) [12]. Despite SiC's advantages, Sapphire still continues to be a popular substrate because of its significantly lower cost. Another low cost alternative that has been researched is Si. Si substrates not only offer a low cost alternative with roughly one half the thermal conductivity of SiC but also allow the potential integration of power

electronics on an advanced and mature Si technology [13]. Other substrate candidates that have been investigated include Lithium Gallate [14] and Neodymium Gallate [15].

D. POLARIZATION EFFECTS

Certain molecular crystals become polarized when they are mechanically stressed (Figure 5) [16]. When the atoms are pushed from their natural positions, their charges do not balance appropriately. As a result, surface charges appear and a voltage difference between the two crystal faces is produced. These same crystals will also exhibit mechanical strain or distortion when they experience an electric field. The direction of distortion will depend upon the direction of the electric field or polarity of the applied voltage. These characteristics describe the PZ effect inherent to these crystals.

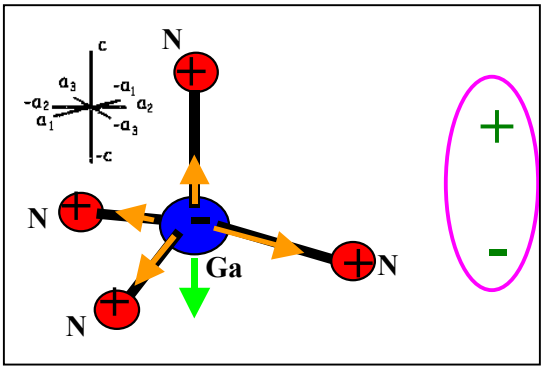

Figure 5. Vertical stress applied to Wurtzite GaN molecule and resultant polarization.

Only crystals, such as group III-nitrides, without a center of symmetry, called noncentrosymmetric, can exhibit PZ properties. In addition to the strain-induced PZ polarization, calculations have shown that group III-nitrides have strong spontaneous polarization [17][18]. In GaN, it can be seen that the direction of polarization is along the c-axis from N to Ga (Figure 5). The direction of a device's polarization, Ga- or N-faced, is very important because it will determine where the 2DEG will form in a HEMT.

The face type of a GaN-based device determines the location of the 2DEG but the percentage of aluminum (Al) determines the charge density in AlGaN/GaN HEMT's. Studies have shown a direct relationship between the concentration of Al in the AlGaN

layer to sheet charge density at the interface [19] because AlGaN has a different lattice constant than GaN and in-plane biaxial stress is created when AlGaN is grown on GaN (Figure 6) [20]. This is the manifestation of the piezoelectric effect in an AlGaN/GaN HEMT.

GaN and its compounds have high piezoelectric properties that result in measurable electric fields in the mega-Volts per centimeter range. These high electric fields effect conductivity, allowing for electron transport without using dopants [1].

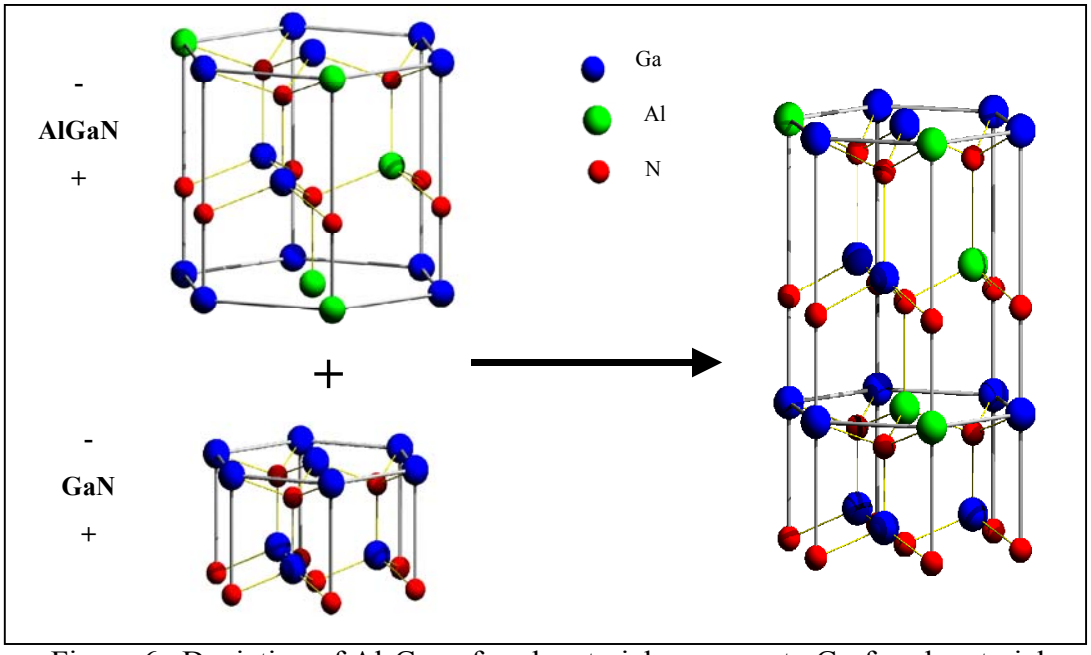

Figure 6. Depiction of Al_xGa_{1-x}-faced material grown onto Ga-faced material. (Negative charge is vertically up, positive charge is vertically down)

Much of the past research into the polarization, PZ and spontaneous, properties between AlGaN and GaN layers has focused on the internal molecular strain caused by their lattice mismatch (Figure 7). Of course, the amount of external stress or strain is another area of research and factor to consider in the accurate evaluation of AlGaN/GaN semiconductor performance.

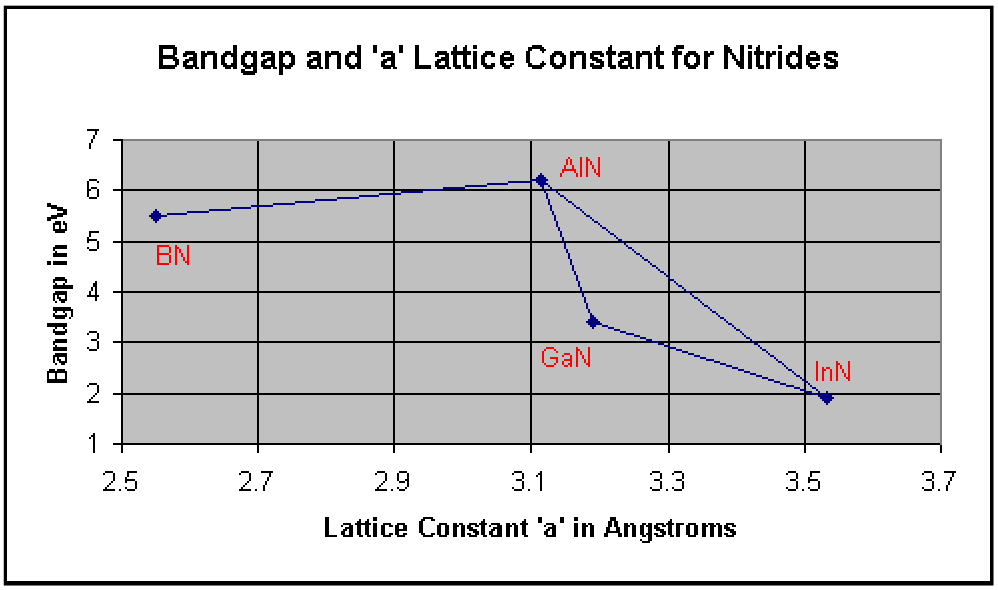

Figure 7. Bandgaps and lattice constants for select semiconductor compounds.

Additionally, an applied electric field might influence the PZ effect. In simplistic terms, piezoelectric crystals are electromechanical transducers that change strain into electric potential and vice versa. Theoretically, the application of an external electric field will cause some mechanical/physical deformation that could further affect the total PZ effect. Another potentially important parameter is thermal expansion strain. Further research into developing reliable relationships between layer microstructure and thermal strain is needed to potentially include this parameter in future modeling.

THIS PAGE INTENTIONALLY LEFT BLANK

III. DEVICE MODELING AND SIMULATION

A. SILVACO

Silvaco International produced the device modeling and simulation software utilized in this work. Silvaco's ATLAS™ is a versatile and modular program designed for one, two, and three-dimensional device simulation. BLAZE™ and GIGA™, ATLAS™ sub-modules (Figure 8), perform specialized functions required for advanced materials, heterojunctions, and temperature-dependent conditions. To control, modify, and display the modeling and simulation, the Virtual Wafer Fabrication (VFW) Interactive Tools, namely DECKBUILD™ and TONYPLOT™, were utilized (Figure 9).

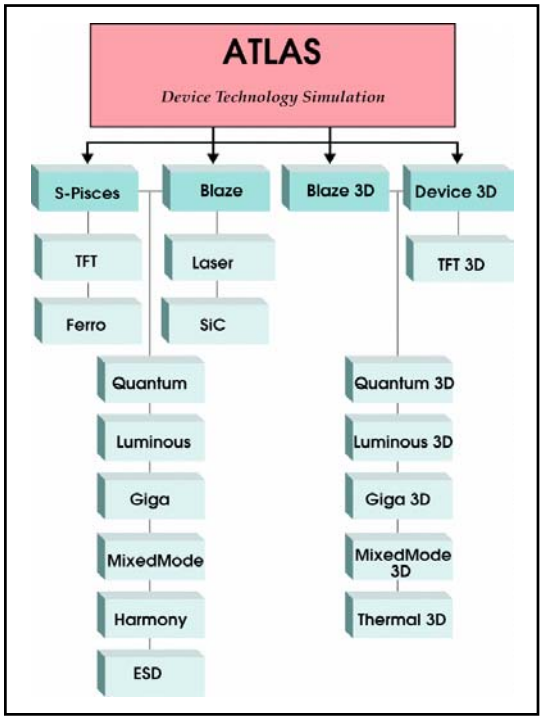

Figure 8. Representation of ATLAS' modular structure.

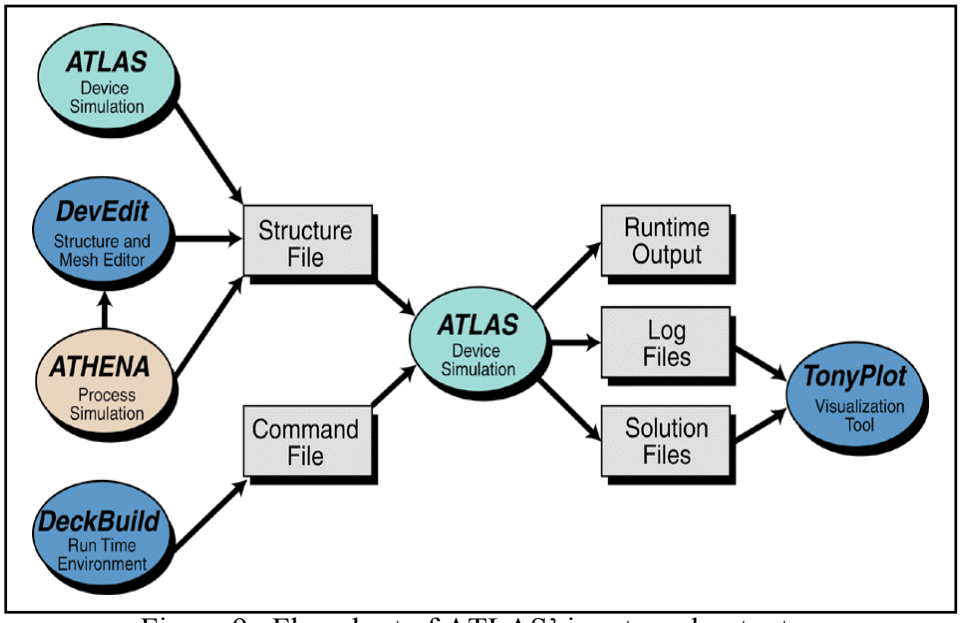

Figure 9. Flowchart of ATLAS' inputs and outputs.

Unlike some other modeling software, Silvaco uses physics-based simulation rather than empirical modeling. In truth, empirical modeling produces reliable formulas that will match existing data but physics-based simulation predicts device performance based upon physical structure and bias conditions. To perform the modeling, the Silvaco software graphically represents a device on a two-dimensional grid with designated electronic meshing parameters. At every mesh intersection, the program simulates carrier transport by means of differential equations derived from Maxwell's laws. To achieve accuracy, the program incorporates the appropriate physics via numerical procedures.

To accurately model the III-V semiconductors, ATLAS must employ the BLAZE program extension to modify calculations that involve energy bands at heterojunctions. The heterojunctions require changes in calculating current densities, thermionic emissions, velocity saturation, and recombination-generation.

ATLAS attempts to find solutions to carrier parameters such as current through electrodes, carrier concentrations, and electric fields throughout the device. ATLAS sets up the equations with an initial guess for parameter values then iterates through parameters to resolve discrepancies. ATLAS will alternatively use a decoupled (Gummel) approach or a coupled (Newton) approach to achieve an acceptable

correspondence of values. When convergence on acceptable values does not occur, the program automatically reduces the iteration step size. ATLAS generates the initial guess for parameter values by solving a zero-bias condition based on doping profiles in the device.

B. PRIOR SILVACO MODELING EFFORTS

Other efforts have been performed to model AlGaN/GaN HEMT's. Three such efforts have been conducted by Naiqian Zhang [21] and Shreepad Karmalkar [7] of the University of California at Santa Barbara (UCSB) and Karl Eimers [1] of the Naval Postgraduate School (NPS).

1. Surface Donor-Like States Approach

In [21] and [7], UCSB follows Ibbetson's theory [22] of surface donor-like states being the source of the electrons for the HEMT's 2DEG and, as a result of the strong internal electric field, the electrons are driven into the quantum well. Using this concept and the simplified approach to the HEMT's charge distribution in equation (1),

$$n_s = n_f = n_{p+} - n_{p-} + n_t + n_d = n_t + n_d \qquad (1)$$

where, n_s is the channel electron concentration; n_f is the electron sheet concentration; n_{p+} and n_{p-} are polarization dipole charges at opposite faces of the AlGaN layer; n_t is the insulator-donor layer interface charge; and n_d is the ionized unintentional doping charge, both [21] and [7] attained results comparable with experimental data for unintentionally-doped and field plate HEMT's, respectively. This simplified approach does not consider the spontaneous and piezoelectric-based charges separately.

2. C-Interpreter Approach

In [1], Eimers uses Ambacher's [23] equations (Table 2) in ATLAS' C-INTERPRETER to model the carriers' characteristics in the $Al_xGa_{1-x}N$/GaN HEMT (Al mole fraction x = 0.3).

	EQUATIONS
Sheet electron concentration	$n_S(x) = \frac{\sigma(x)}{e} - \left(\frac{\varepsilon_0 \varepsilon(x)}{d_{AlGaN} e^2}\right)\left[e\phi_b(x) + E_F(x) - \Delta E_C(x)\right]$
Dielectric constant	$\varepsilon(x) = -0.3x + 10.4$
Work function	$e\phi_b = (1.3x + 0.84)eV$
Conduction band offset	$\Delta E_C = 0.7\left[E_g(x) - E_g(0)\right]$
Bandgap	$E_g(x) = (x6.13 + (1-x)3.42 - x(1-x)1.0)eV$
PZ effect polarization	$P_{PE} = 2\{r(x)-1\}\left\{\frac{a_0(x) - a(GaN)}{a_0(x)}\right\}\left(e_{31}(x) - e_{33}(x)\frac{C_{13}(x)}{C_{33}(x)}\right)$
Lattice constant	$a_0(x) = (-0.077x + 3.189)10^{-10}\, m$
Elastic constant	$C_{13}(x) = (5x + 103)GPa$
Elastic constant	$C_{33}(x) = (-32x + 405)GPa$
Piezoelectric coefficients	$e_{ij}(x) = \left(e_{ij}(AlN) - e_{ij}(GaN)\right) * x + e_{ij}(GaN)$
Spontaneous Polarization	$P_{SP}(x) = (-0.052x - 0.029)\frac{C}{m^2}$
Degree of Relaxation	$r(x) = \begin{cases} 0 & 0 \le x < 0.38 \\ 3.5x - 1.33 & 0.38 \le x \le 0.67 \\ 1 & 0.67 < x \le 1 \end{cases}$
Sheet charge	$\sigma(x) = \{P_{PE}(bottom) + P_{SP}(bottom)\} - \{P_{PE}(top) + P_{SP}(top)\}$
Fermi level	$E_F(x) = -0.102967 + (2.1917)x - (7)x^6$

Table 2. Equations utilized in [1].

Eimers concentrated on utilizing these equations in ATLAS' C-INTERPRETER in conjunction with a DEVEDIT-generated HEMT model to simulate the polarization effects and electron sheet concentration within the transistor. Despite DEVEDIT's inability to recognize AlGaN as a material, Eimers was able to modify the program's material properties for AlN to approximate AlGaN. Figure 10 is a representation of the resultant IV curves for 0V, -1V, -3V, and -5V gate bias with drain voltage being ramped from 0V to 20V. Figure 11 displays the experimentally derived IV curves for the doped AlGaN/GaN HEMT.

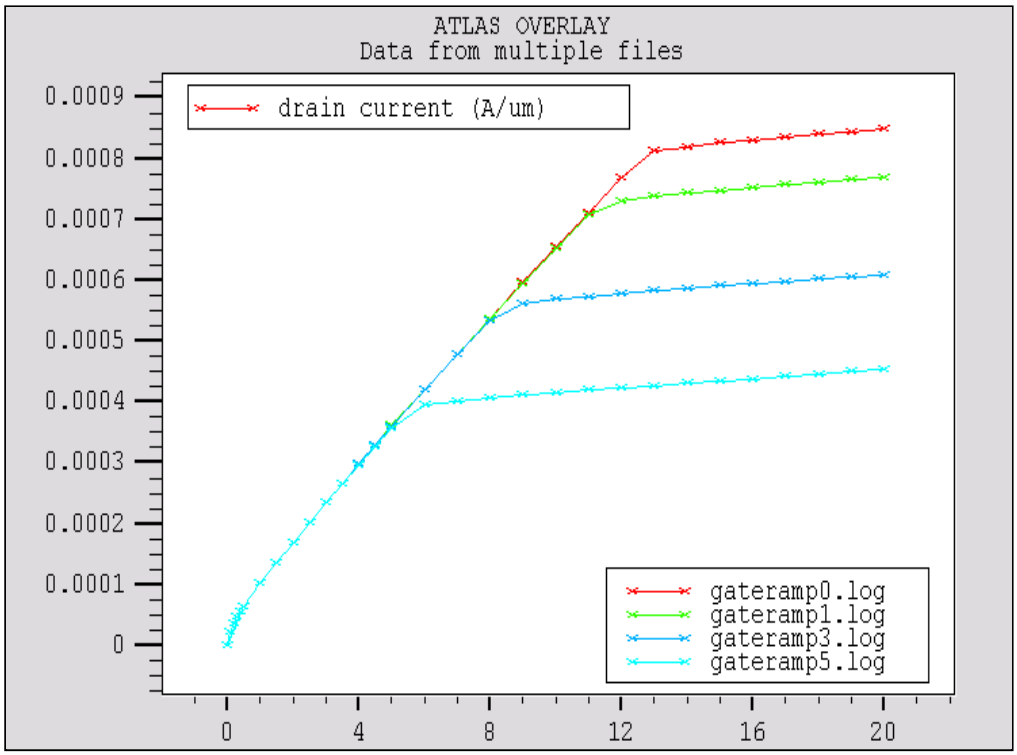

Figure 10. Simulated IV curves for doped AlGaN/GaN HEMT. (From: [1])

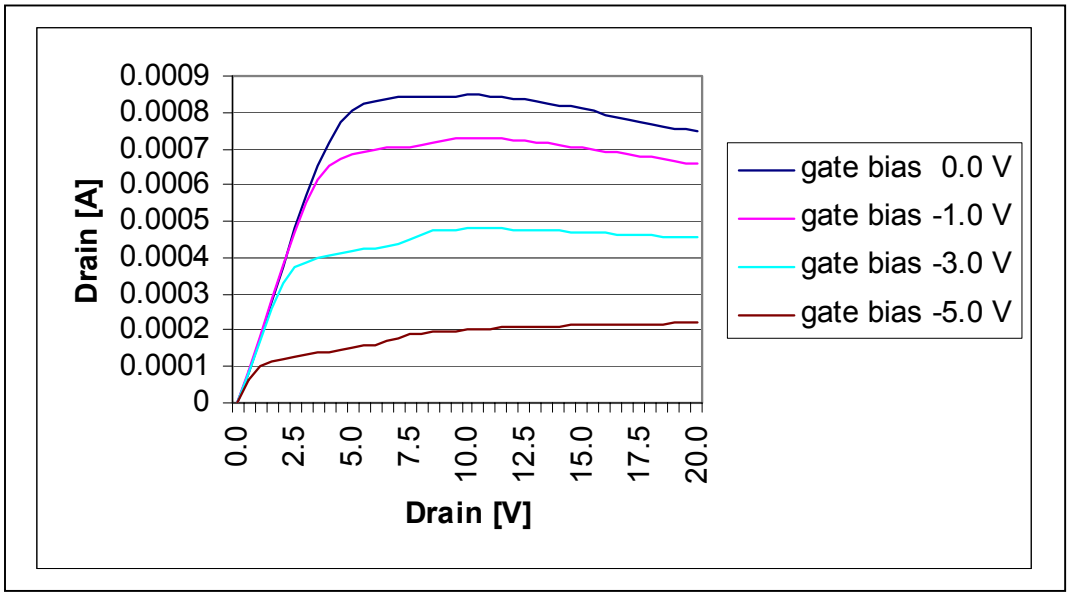

Figure 11. Experimentally derived IV curves for doped AlGaN/GaN HEMT. (From: [1])

The modeled IV curves had noticeable differences. Despite the differences, the modeled and experimental curves were roughly similar. This demonstrated the potential for using the Silvaco software installed on a UNIX system, specifically the C-INTERPRETER, to model doped HEMT's.

C. THIS EFFORT

This work focuses on an $Al_{0.3}Ga_{0.7}N$/GaN HEMT that was constructed and physically tested by S. C. Binari (et al.) at the Naval Research Laboratory (NRL) in Washington, D.C. and is the second approach by NPS to model this HEMT. Figure 12 is a representation of a HEMT tested in [24] and Figure 13 is the ATLAS-generated representation of the HEMT.

Noted, the model appears different from the tested HEMT. First, the source and drain contacts were placed on the sides of the AlGaN and GaN layers to allow proper current flow from contacts to the device. The change in the contact placement is required because the software treats the AlGaN layer as an effective insulator preventing any current flow. In addition, the implant damage zones, which provide isolation in the real device, were not included.

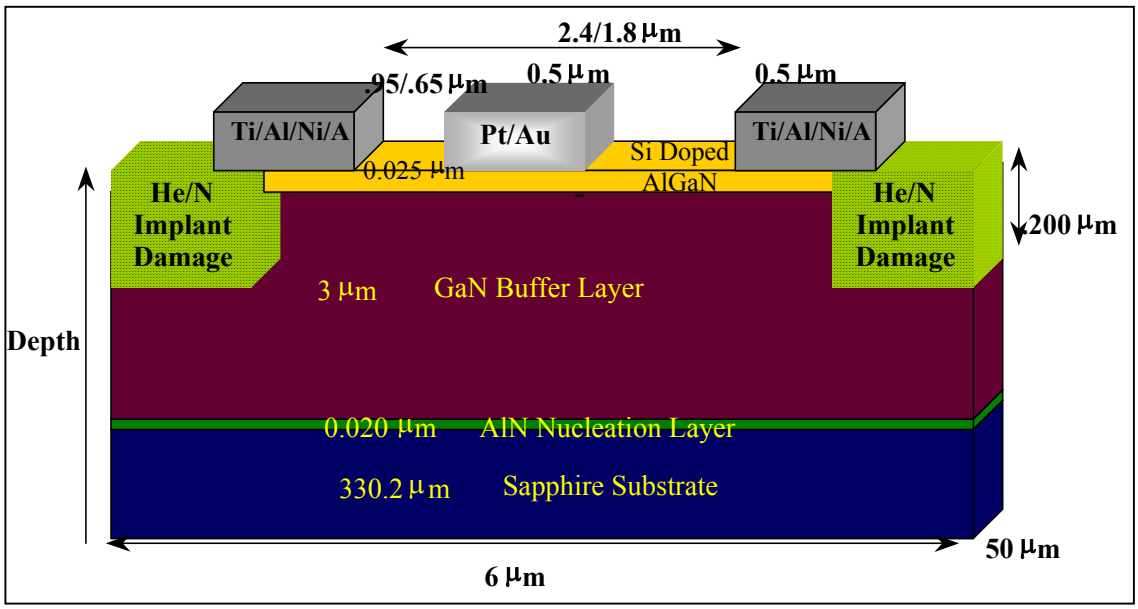

Figure 12. Representation of NRL's doped AlGaN/GaN HEMT.

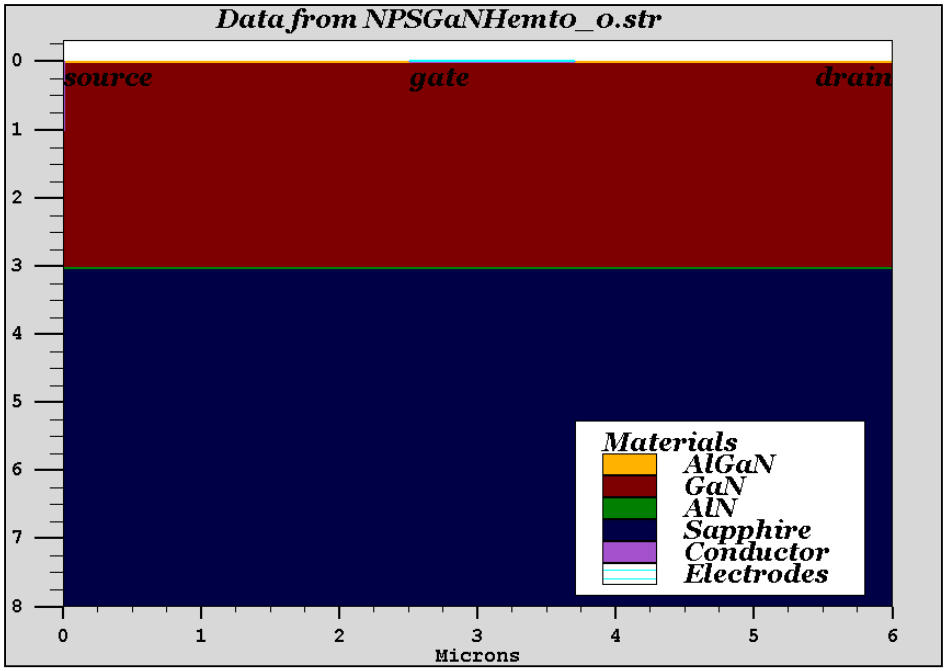

Figure 13. ATLAS-generated representation of NRL's doped AlGaN/GaN HEMT

For modeling purposes, this work proceeded using an approach aimed at representing the HEMT layers, AlGaN and GaN, as dipoles. With this dipole approach, we assumed Ga-faced and AlGa-faced layers, respectively. To simulate the HEMT's characteristic 2DEG and polarization, the AlGaN layer is n-doped 5e+18 from the top of the layer to 0.005 microns then p-doped 5e+18 from 0.019 to 0.024 microns, and the GaN layer is n-doped 2e+19 from 0.030 to 0.035 microns then p-doped 2e+18 from 3.0 to 3.024 microns (Figure 14, Appendix A). As can be observed, the top layer of electron concentration width in the AlGaN layer is approximately as entered but both the bottom layer of AlGaN hole concentration width and top layer of GaN electron concentration width are decreased due to recombination. Deckbuild's default recombination lifetimes, $1x10^{-7}$ sec, were utilized for this effort. Taking a cutline across this section (vertically

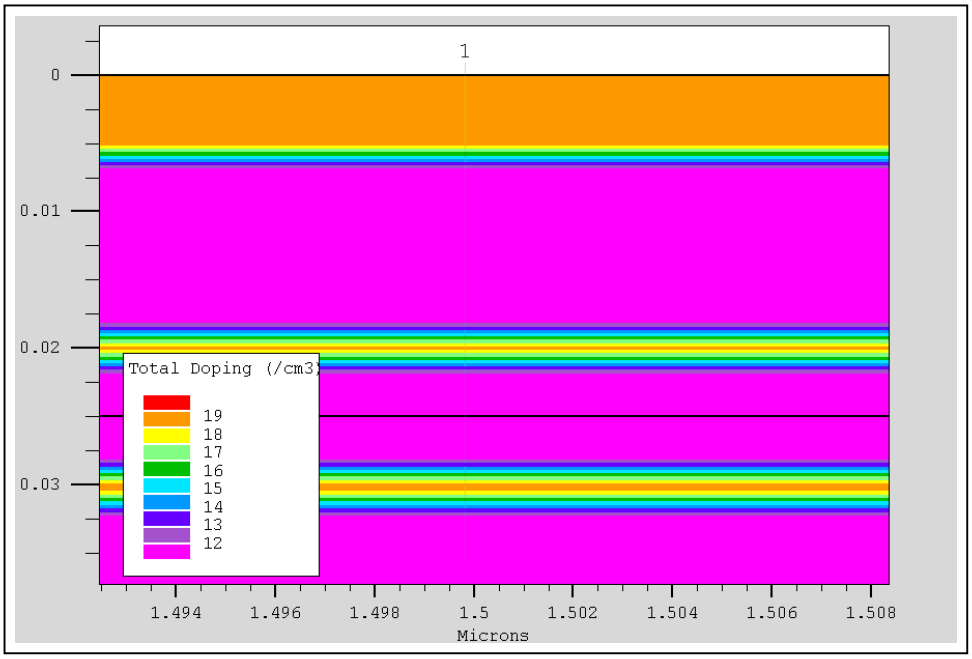

Figure 14. TONYPLOT's representation of doping profile.

down from the "1"), the below electron concentration profile is produced (Figure 15).

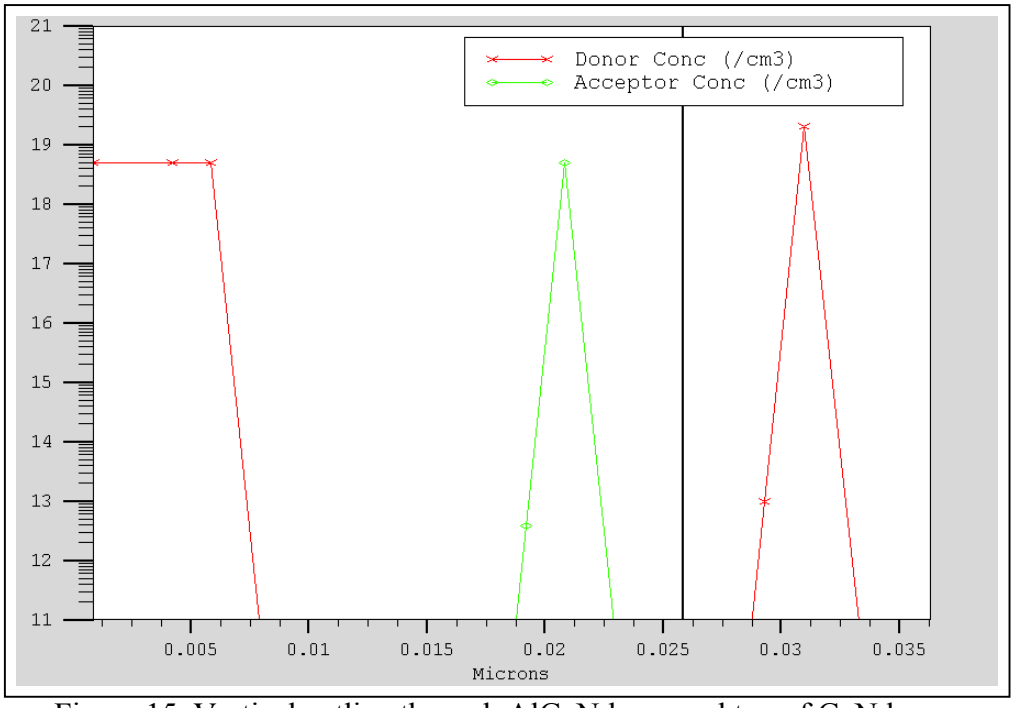

Figure 15. Vertical cutline through AlGaN layer and top of GaN layer.

Taking peak data from Figure 15 and using an algebraic summation similar to equation (1), the result is:

$$(5\text{x}10^{18}\ \text{donors/cm}^2) - (5\text{x}10^{18}\ \text{acceptors/cm}^2) + (1\text{x}10^{19}\ \text{donors/cm}^2) = 1\text{x}10^{19}\ \text{donors/cm}^2$$

This very simple computation does not account for the bottom of the GaN layer because its interaction with the AlGaN layer and top of the GaN layer can be assumed to be negligible (3 μm vice 0.025 μm).

THIS PAGE INTENTIONALLY LEFT BLANK

IV. RESULTS

A. 2-DEG

Making a cutline from the gate at zero bias to the AlN layer, Figure 16 displays the desired spike of electrons on the GaN side of the AlGaN/GaN interface. The dark line is the interface with AlGaN on the left and GaN on the right. The spike in electron concentration (~0.8e+19/cm^3) is representative of the 2-DEG resulting from polarization. Figure 17 is the conduction band energy diagram for zero gate bias. The "dip" or quantum well drops to a –0.05 eV energy level to facilitate electron transport. The HEMT's characteristic quantum well reduces electron scattering and increases electron mobility.

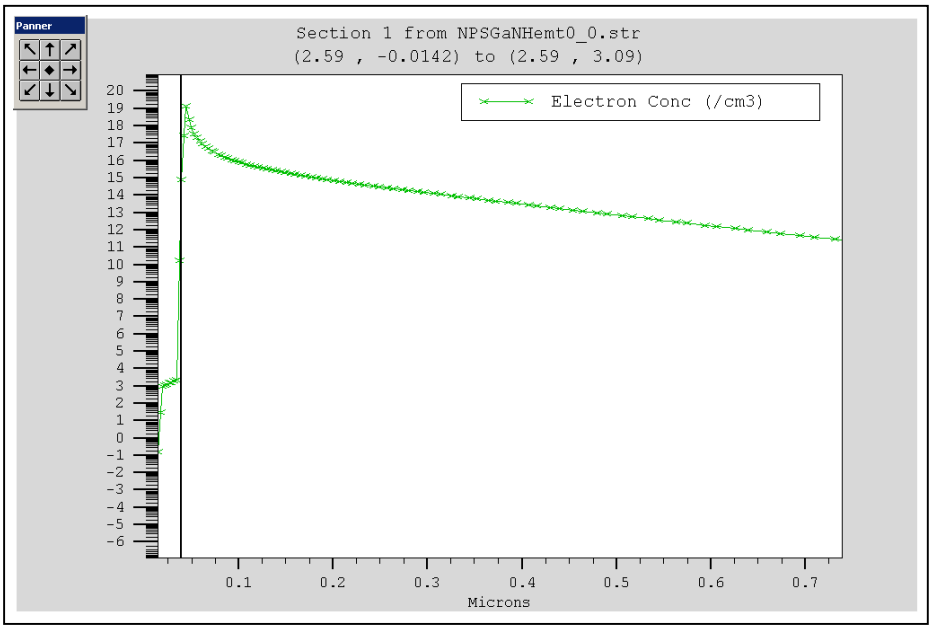

Figure 16. Electron concentration at the AlGaN/GaN interface with zero gate bias.

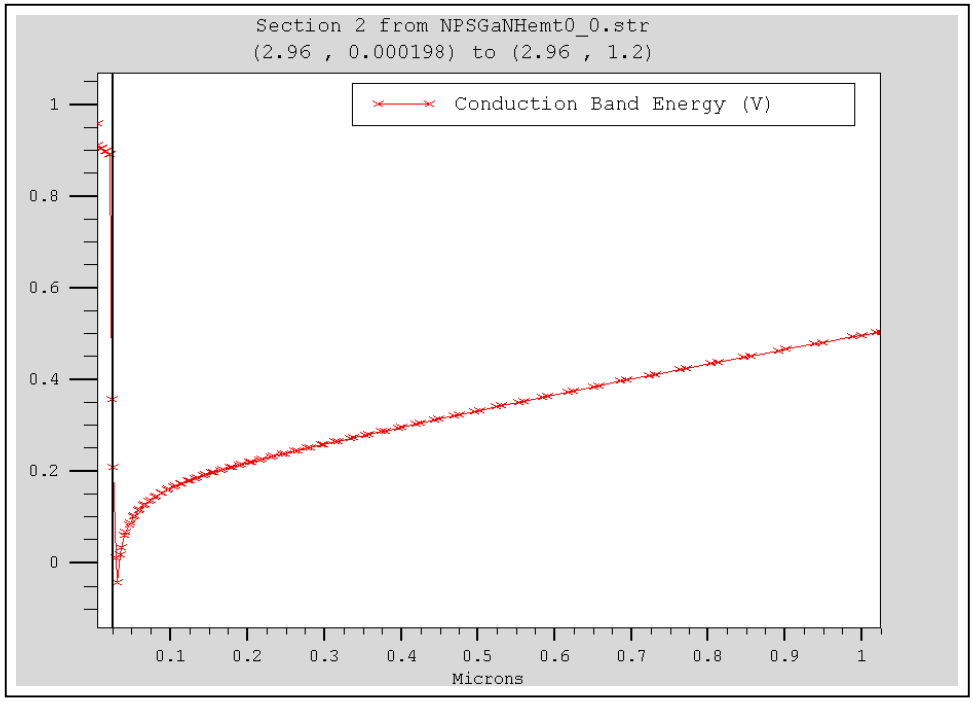

Figure 17. Conduction band diagram showing quantum well at zero gate bias.

B. ELECTRON FLOW

Figures 18-21 are samples of TONYPLOT's representations of the electron concentrations in the AlGaN/GaN HEMT under 0V gate bias and drain voltages 0V and 20V. Graphics for gate biases –1V, -2V, -3V, -4V, and –5V are in Appendix B. These displays will indicate the flow of electrons (and holes) through the HEMT. Figures 18 and 19 are the zero gate bias (V_g) and 0V drain voltage (V_d) condition displays. As can be see, the electron concentration is highest near the AlGaN/GaN interface. In Figure 19, it is clearly shown how the ohmic gate negates the electron concentration. Figures 20 and 21 are the V_g = 0V, V_d = 20V condition graphics. A decreasing electron concentration can be observed below the right side of the gate. This is showing the development of the transistor's depletion region. Figures 22-26 are samples of TONYPLOT's

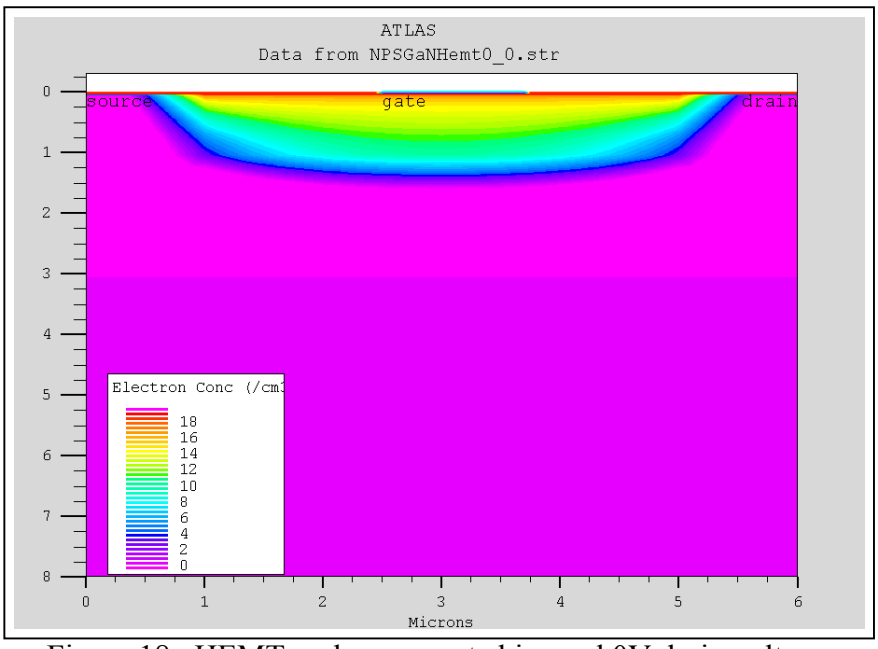

Figure 18. HEMT under zero gate bias and 0V drain voltage.

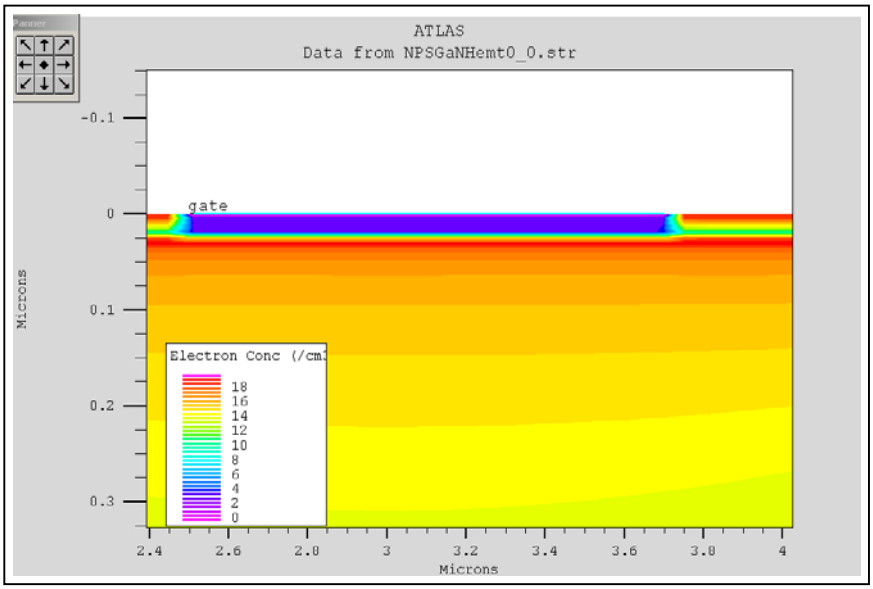

Figure 19. Close-up view of HEMT under zero gate bias and 0V drain voltage.

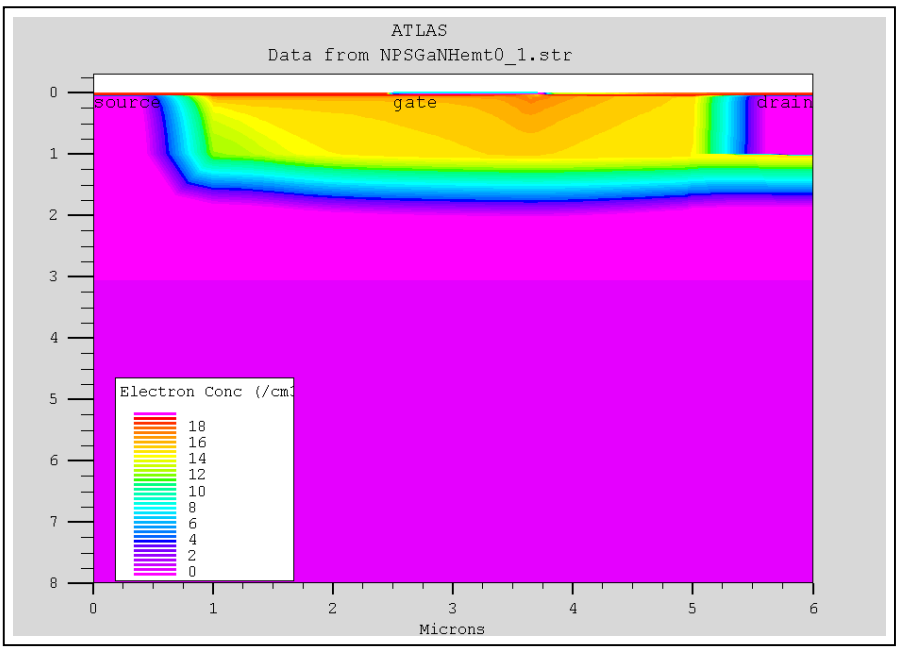

Figure 20. HEMT under $V_g = 0V$, $V_d = 20V$ condition. Depletion region developing.

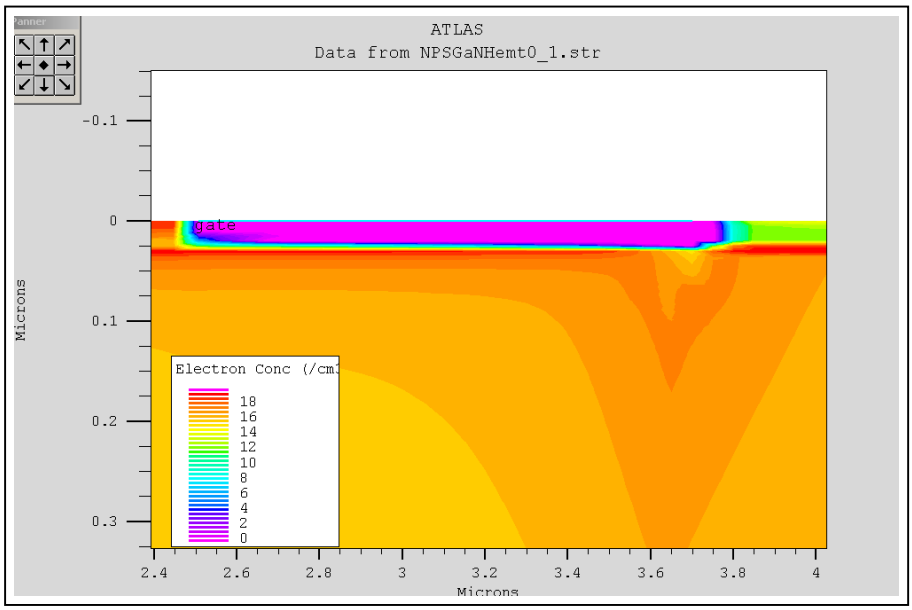

Figure 21. Close-up of HEMT under $V_g = 0V$, $V_d = 20V$ condition.

representations of the current density in the AlGaN/GaN interface under 0V gate bias and drain voltages 0V, 5V, 10V, 15V, and 20V. As can be observed in Figure 22, the region has a positive current density (~3790 A/cm^2). However, after drain voltage increases (Figure 23), a negative current density develops below the interface. This negative current density represents the 2DEG and negative current flow. With increasing drain voltage (Figures 23-26), a decrease and disruption of the negative current flow is shown. The disruption or "pinch off" is caused by the development of the depletion region.

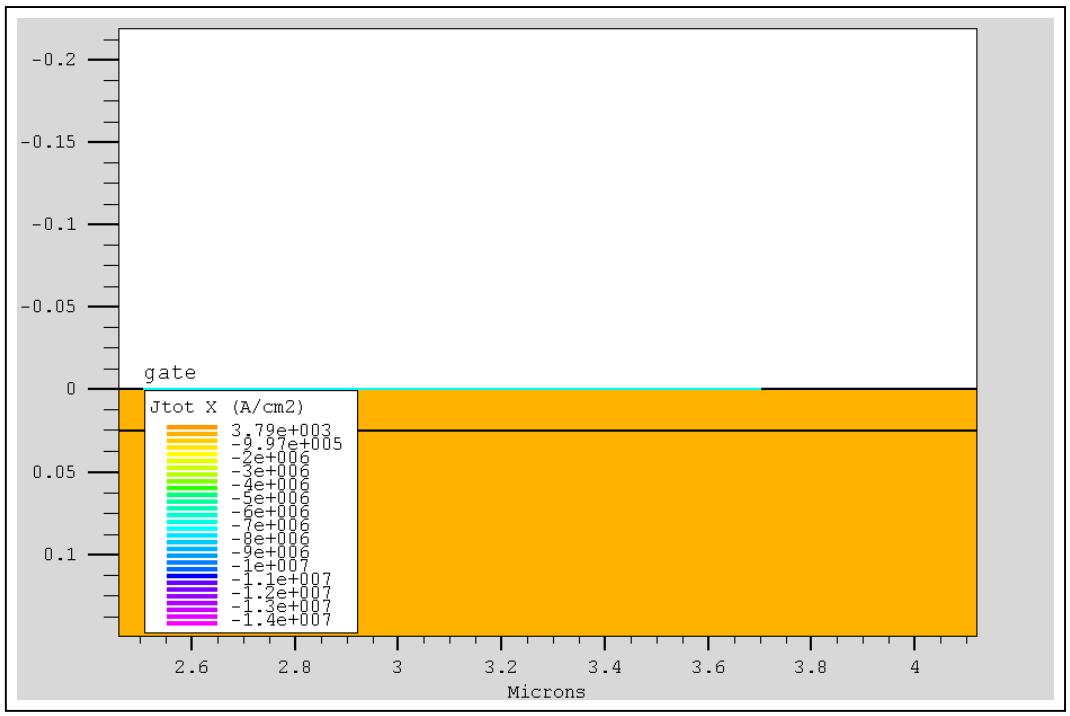

Figure 22. Close-up of HEMT under V_g = 0V, V_d = 0V condition.

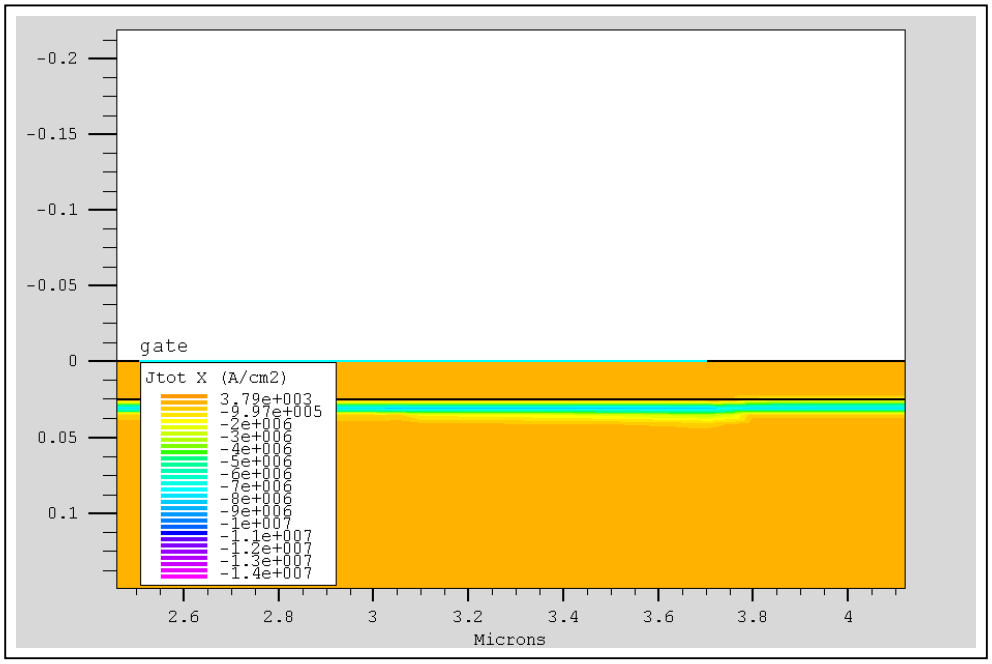

Figure 23. Close-up of HEMT under $V_g = 0V$, $V_d = 5V$ condition.

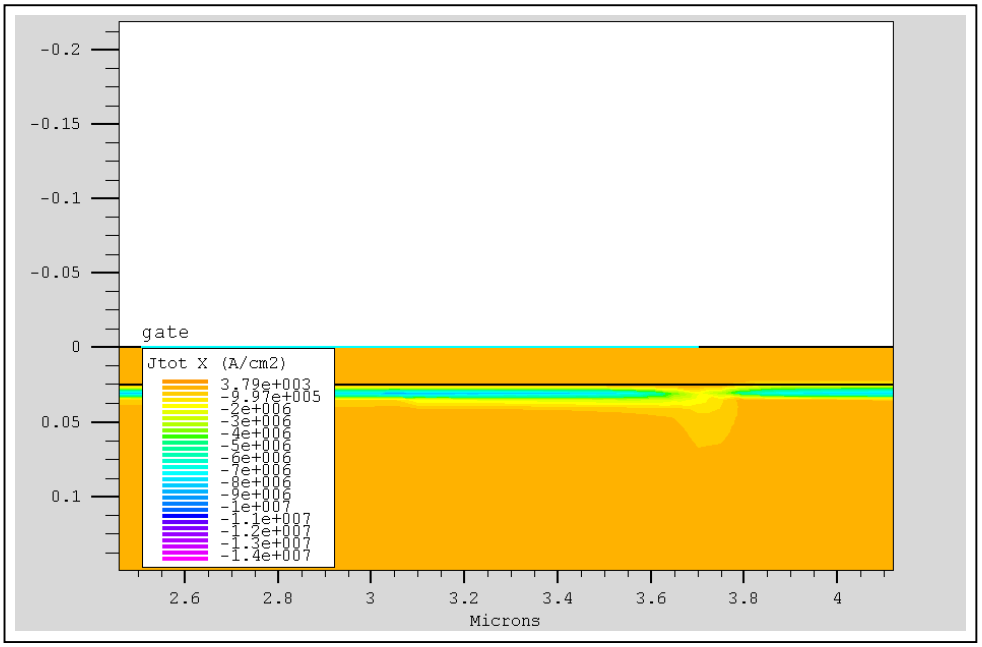

Figure 24. Close-up of HEMT under $V_g = 0V$, $V_d = 10V$ condition.

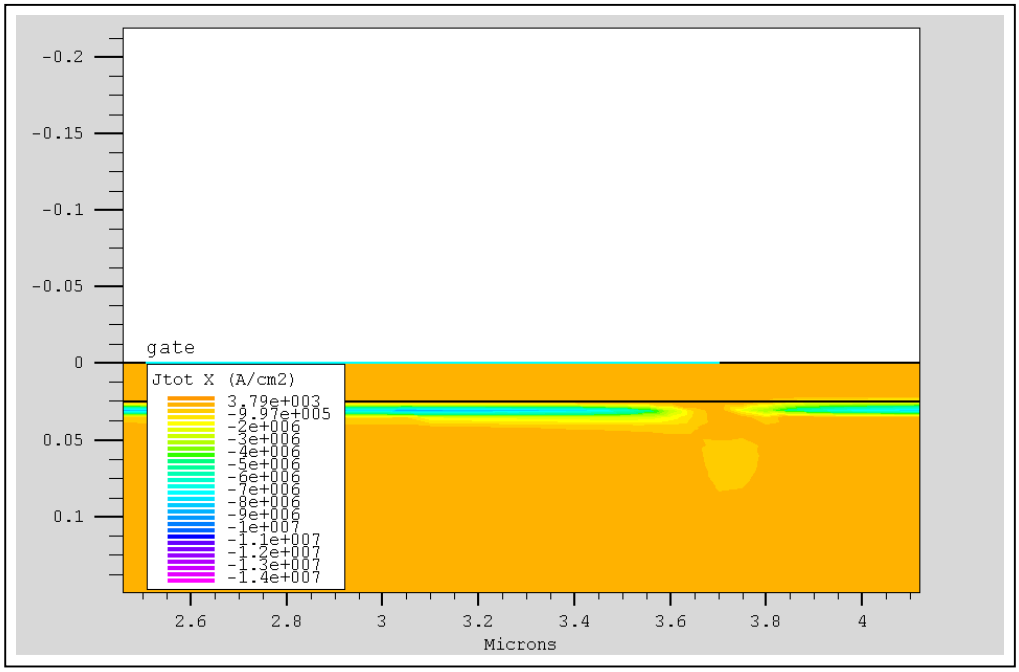

Figure 25. Close-up of HEMT under $V_g = 0V$, $V_d = 15V$ condition.

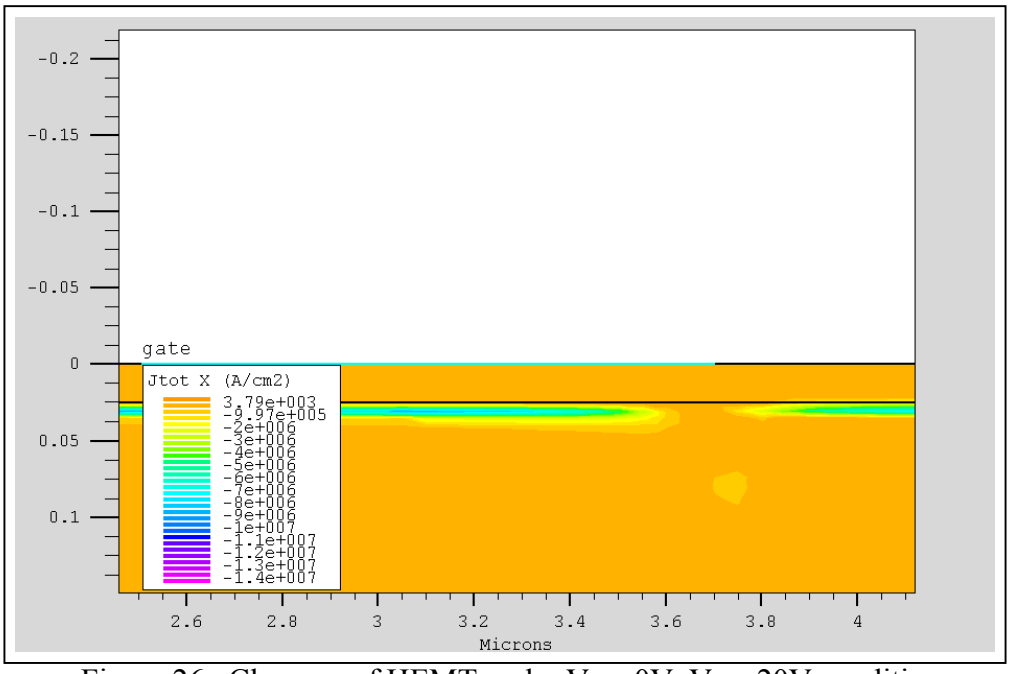

Figure 26. Close-up of HEMT under $V_g = 0V$, $V_d = 20V$ condition.

C. IV CURVES

The $Al_{0.3}Ga_{0.7}N/GaN$ HEMT model was tested and attained the below IV curves for V_g = 0V, -1V, -2V, -3V, -4V, and –5V while ramping V_d from 0-20V (Figure 27). This work's results were compared with NRL's measured results [24](Figure 29) and Eimers' simulated results [1] (Figure 30) for V_g = 0V, -1V, -3V, and –5V (Figure 28).

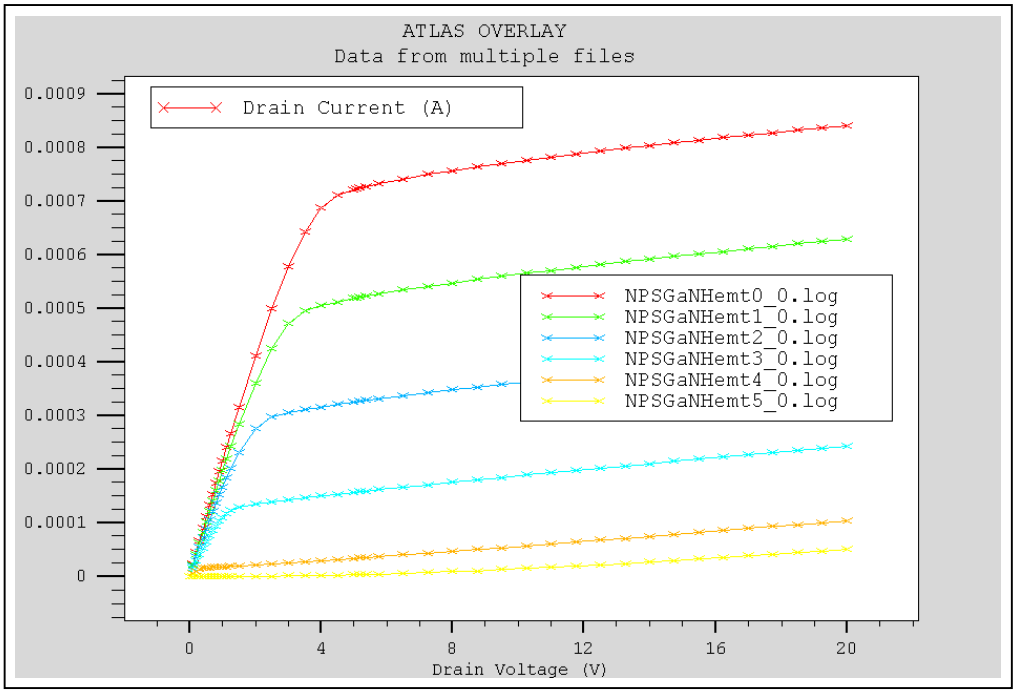

Figure 27. Simulation-generated IV curves for 0V, -1V, -2V, -3V, -4V, and –5V.

In Figures 28 and 29, the "knee" voltages are corresponding ($V_d \approx$ 3V) for the 0V and –1V curves. In addition, the slope of the 0V, -1V, -3V curves ($\approx$0.2 mA/V) show strong correlation. The dissimilarities noted are the "shortfalls" on the curve peaks and the current collapse. The peak "shortfalls" appear to be a result of the depletion region's growth in the simulation. Multiple modifications to the gate's work function did not resolve this occurrence. The current collapse in the experimental curves was theorized to

be a result of GaN defect traps [24]. Binari considered the graphically-displayed current collapse to be consistent with the observed correlation between the amount of current collapse and resistivity of the buffer layer. Defect traps were not simulated in this work thus the program was unable to compensate for these potential effects. Figure 31 is an overlap of NRL's and this work's IV curves for V_g = 0V, -1V, -3V, and –5V.

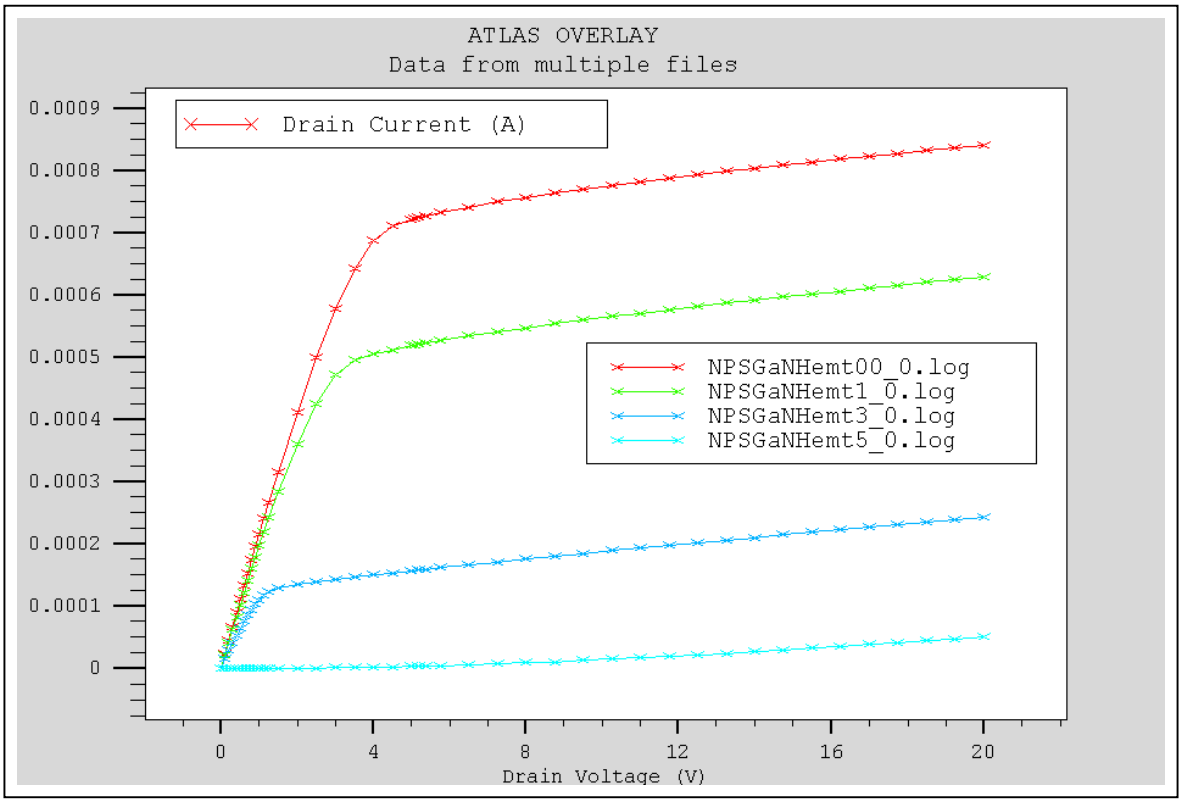

Figure 28. Simulation-generated IV curves for 0V, -1V, -3V, and –5V gate bias.

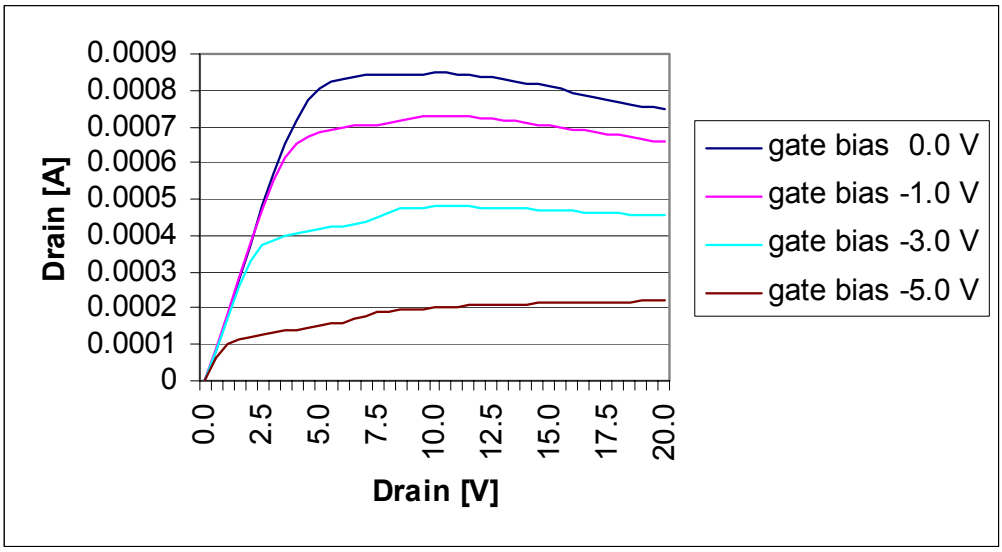

Figure 29. NRL's derived IV curves for 0V, -1V, -3V, and –5V gate bias. (From: [1])

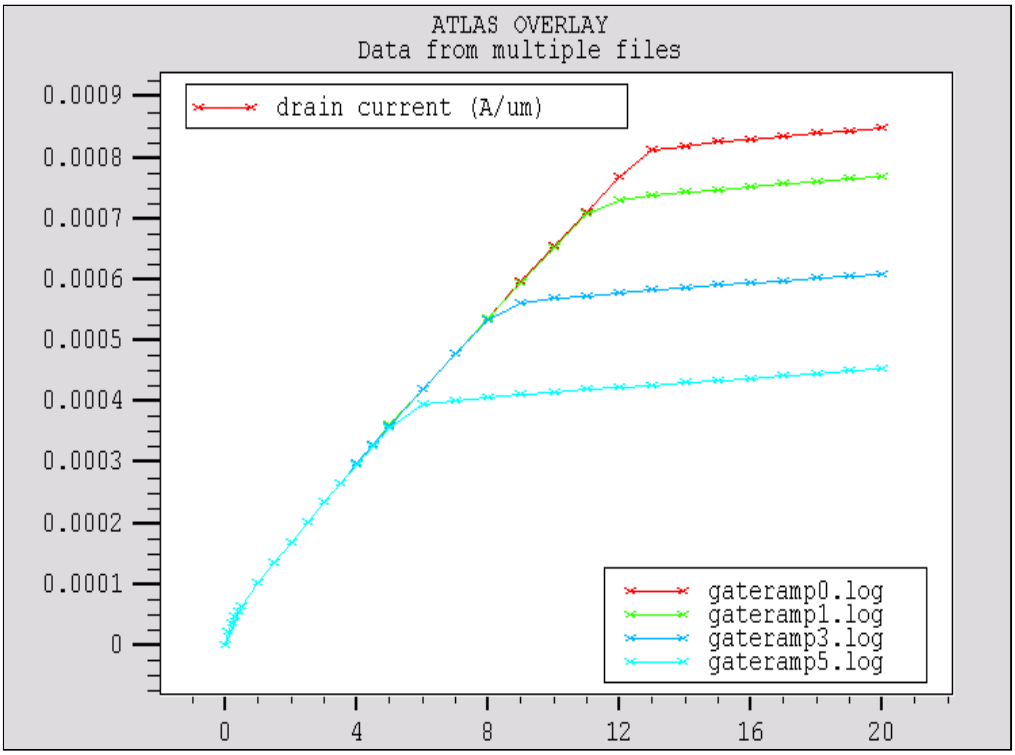

Figure 30. Eimers' simulated IV curves for 0V, -1V, -3V, and –5V gate bias. (From: [1])

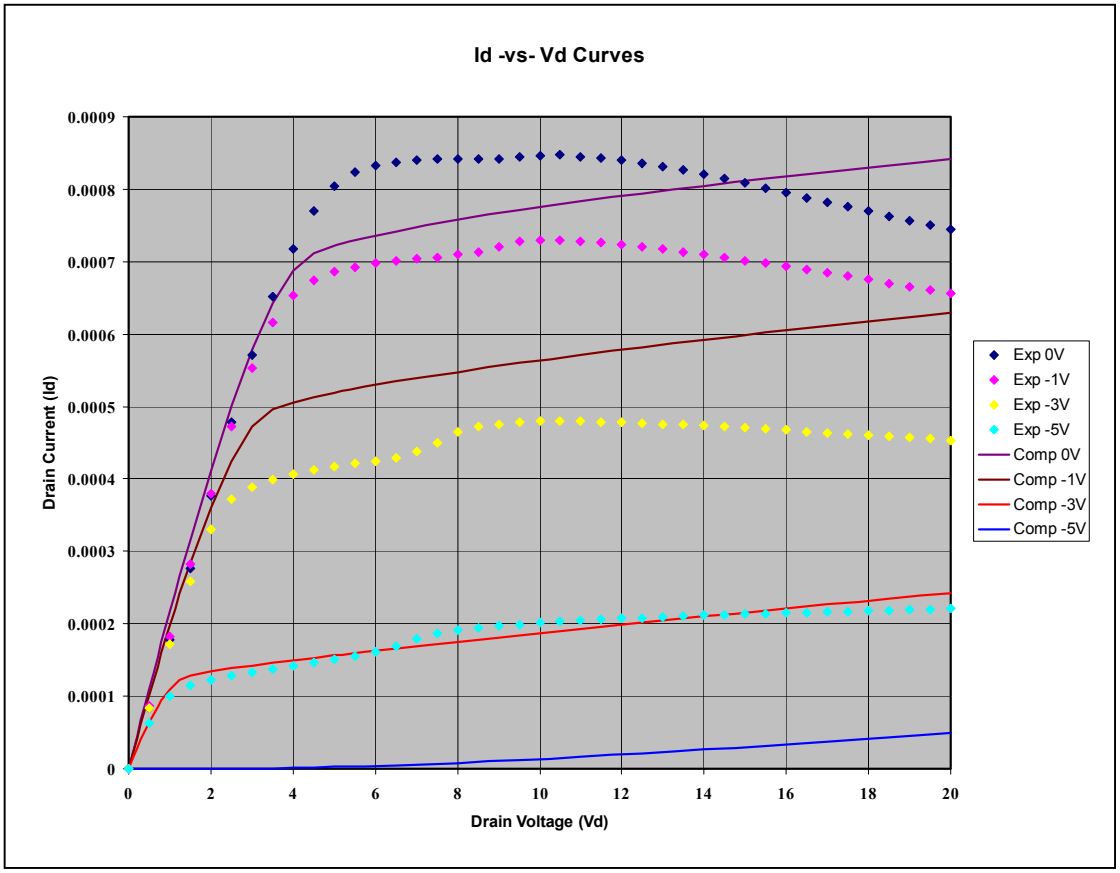

Figure 31. Overlap of NRL's and this work's IV curves for V_g = 0V, -1V, -3V, and –5V.

Appendix C contains transconductance and subthreshold plots of the $Al_{0.3}Ga_{0.7}N/GaN$ HEMT. As can be observed in Figure C1, threshold voltage is approximately –4.5 volts. Experimental curves of these were not available thus no comparison was performed.

THIS PAGE INTENTIONALLY LEFT BLANK

V. CONCLUSIONS AND RECOMMENDATIONS

A. CONCLUSIONS

The polarization, piezoelectric and spontaneous, effects are significant in AlGaN/GaN devices and can be modeled with some degree of accuracy utilizing the Silvaco software. In this work, the desired density of carriers has been demonstrated to concur with established theory by performing the modeling using a dipole approach. Also, the current versus voltage performance (IV curves) of the modeled device approximates a measured device to a degree of accuracy.

Nevertheless, the model requires greater refinement and treatment to more closely match actual device performance. Some potential areas for cause and correction of the inaccuracies have been previously outlined. In addition to these, other potential methods to resolve the IV curve discrepancies are currently available in the Silvaco software. Some of methods include modeling the thermal, interface, and quantum effects related to the device and its environment. The Silvaco software has a sub-program, GIGA^{TM}, which extends ATLAS^{TM} to account for heat transfer at the lattice-level by implementing Wachutka's thermodynamic model. Also, ATLAS^{TM} has an INTERFACE statement that allows one to define the interface charge density. This function might allow for a simple method for defining the 2-DEG but it could modify the surface recombination velocity and thermionic emissions, which might be undesirable. The quantum effects can be addressed in Silvaco by solving Schrodinger's equation, which will modify the normally calculated density of states and carrier concentrations.

This work reported mainly the results derived from a ATLAS program that had the piezoelectric and spontaneous polarizations entered as a combination (Appendix A). However, the same results were attained using a program which algebraically separated the polarizations (Appendix D).

B. RECOMMENDATIONS

Strenuous and concentrated efforts should be placed on modeling a closer match to real device performance. Revisit the C-INTERPRETER approach to modeling using some lessons learned from this work because, once it is refined, the C-INTERPRETER method should provide greater flexibility for various HEMT's and conditions.

Work closer with Silvaco to incorporate the piezoelectric and spontaneous polarization effects into their modeling software. This would aid the Navy in researching and developing newer GaN devices. Additionally, investigation into the possibility of modeling the dynamic effects between the external stress, applied voltage bias, and polarization effects should occur.

For Naval Postgraduate School (NPS) Electrical Engineering students, an introduction to Silvaco's modeling software at the NPS undergraduate-course level. This would provide students and staff with additional corporate knowledge on a software package that is currently being employed by sponsors, such as the Navy Research Laboratory, the Space and Warfare Command, and other institutions involved with semiconductor research.

LIST OF REFERENCES

1. Eimers, Karl P., "2D Modeling of GaN HEMTs Incorporating the Piezoelectric Effect," Thesis, Naval Postgraduate School, March 2001
2. Smith, M.C., Dunleavy, L.P., "Comparison of Solid State, MPM, and TWT Based Transmitters for Spaceborne Applications," Proceedings of IEEE Southeastcon '98, pp. 256-259, April 23, 1998.
3. Gonzalez, Guillermo, *Microwave Transistor Amplifiers: Analysis and Design*, Prentice Hall, New Jersey, 1997, p. 81.
4. Shinohara, Keisuke, et al, "Extremely High-Speed Lattice-Matched InGaAs/InAlAs High Electron Mobility Transistors with 472 GHz Cutoff Frequency," Jpn. J. Appl. Phys. Vol. 41 (2002) L437-L439 Part 2, No. 4B, 15 April 2002
5. Albrecht, John D., et al, "AlGaN/GaN Heterostructure Field-Effect Transistor Model Including Thermal Effects," *ELECTRON DEVICES*, November 2000, Vol. 47, No. 11.
6. Karmalkar, Shreepad, et al, "Enhancement of Breakdown Voltage in AlGaN/GaN High Electron Mobility Transistors Using a Field Plate," *ELECTRON DEVICES*, Aug 2001, Vol. 48, No.8, pp. 1515-1521.
7. Pierret, Robert, *Semiconductor Device Fundamentals*, Addison-Wesley Publishing Company, Massachusetts, 1996, p. 526.
8. Dimitrijev, Sima, *Understanding Semiconductor Devices,* Oxford University Press, New York, 2000.
9. Saxler, A., et al, "Electrical transport of an AlGaN/GaN two-dimensional electron gas," internet, nsr.mij.mrs.org/5S1/W11.10/article.pdf
10. Jelenski, Andrzej, "Gallium Nitride--New Material for Microwave and Optoelectronics," Microwaves and Radar, MIKON '98, 12th International Conference on , Vol. 4, 1998, pp. 147-158.
11. Burm, J., "General Remarks on GaN-based Transistors and Potential for High Temperature/Power Operation," Jun 1998, *Properties, Processing and Applications of Gallium Nitride and Related Semiconductors,* INSPEC 1999, p. 569.
12. Eastman, Lester F., "High Power, Broadband, Linear, Solid State Amplifier," MURI 14th Quarterly Report, March 2000
13. Chumbes, Eduardo M., et al, "AlGaN/GaN High Electron Mobility Transistors on Si(111) Substrates," *ELECTRON DEVICES*, 3 March 2001, Vol. 48, No.3, pp. 420-426.
14. Doolittle, W.A., et al, "Recent Advances in III-Nitride Devices Grown on Lithium Gallate," *physica status solid*, Vol. 188, Issue 2, pp. 491-495.

15. "Substrates Materials for GaN," internet, www.itme.edu.pl/z18/ substrates_gan.html

16. Kasap, S.O., *Principles of Electrical Engineering Materials and Devices,* IRWIN, Chicago, IL, 1997.

17. MRS Internet J. Nitride Semicond. Res. 4S1, G8.4(1999).

18. F. Bernardini, et al, *Phys. Rev.* B 56, 16(1997).

19. Asbeck, P.M., et al, "Piezoelectric Charge Densities in AlGaN/GaN HFETs," *ELECTRONIC LETTERS*, 3 July 1997, Vol. 33, No.14, pp. 1230-1231.

20. Petrosky, K.J., "High-Power High-Frequency SiC and GaN Devices for Microwave Amplifier Applications," 12 March 2002, GOMAC Conference.

21. Zhang, Naiqian, et al, "Simulation of AlGaN/GaN HEMTs," unpublished report, University of California at Santa Barbara, 2001.

22. Ibbetson, J.P., et al, "Polarization effects, surface states, and the source of electrons in AlGaN/GaN heterostructure field effect transistors," *Applied Physics Letters*, 10 July 2000, Vol. 77, No.8, pp. 250-252.

23. Ambacher, O., et al, "Two Dimensional Electron Gases Induced by Spontaneous and Piezoelectric Polarization in Undoped and Doped AlGaN/GaN Heterostructures," *Journal of Applied Physics,* Vol. 87, Number 1, January 1, 2000, p. 334-344.

24. Binari, S.C. et al, "Trapping Effects and Microwave Power Performance in AlGaN/GaN HEMTs," *Electron Devices*, 3 March 2001, Vol. 48 No. 3, pp. 465-471

APPENDIX A. DECKBUILD SIMULATION INPUT DECK

```
go atlas
Title    AlGaN/GaN HEMT with AlN Nucleation Layer
#        based upon NRL experimental HEMT (0.3 Al mole fraction)
#         Vg = 0V
#
#
# SECTION 1: Meshing Parameters
#
mesh

x.mesh loc=0.0  spac=1.0
x.mesh loc=1.0  spac=0.1
x.mesh loc=3.0  spac=0.05
x.mesh loc=5.0  spac=0.05
x.mesh loc=6.0  spac=1.5

y.mesh loc=0.0    spac=0.005
y.mesh loc=0.025  spac=0.005
y.mesh loc=1.0   spac=0.05
y.mesh loc=3.025  spac=2.0
y.mesh loc=3.055  spac=2.0
y.mesh loc=8.0    spac=3.0
#
#
# SECTION 2: Structure Specification
#
region     num=1  material=AlGaN y.min=0.0 y.max=0.025 x.composition=0.3
region     num=2  material=GaN y.min=0.025 y.max=3.025
region     num=3  material=AlN y.min=3.025 y.max=3.045
```

```
region     num=4  material=Sapphire y.min=3.045 y.max=8
#
elec       num=1  name=source x.min=0.0 x.max=0.0 y.min=0.0 y.max=1.0
elec       num=2  name=gate   x.min=2.5 x.max=3.7 y.min=-0.5 y.max=0.0
elec       num=3  name=drain  x.min=6.0 x.max=6.0 y.min=0.0 y.max=1.0
#
doping     uniform y.min=0.0 y.max=0.005 n.type conc=5.e18
doping     uniform y.min=0.019 y.max=0.024 p.type conc=5.e18
doping     uniform y.min=0.03 y.max=0.035 n.type conc=2.e19
doping     uniform y.min=3.000 y.max=3.024 p.type conc=2.e18

#
#

#
# SECTION 3: Material Models
#
material material=AlGaN  mun=600 mup=10 affinity=3.82 nc300=2.07e18
material material=AlGaN nv300=1.16e19 eg300=3.96 align=0.8
permittivity=10.32
#
material material=GaN  mun=900 mup=10 nc300=1.07e18
material material=GaN  nv300=1.16e19 eg300=3.4 align=0.8
material material=GaN  arichn=24 arichp=96 edb=0.025 eab=0.160
material material=GaN  permittivity=9.5 vsatn=2e7
#
model material=AlGaN conmob fldmob srh print
model material=GaN conmob fldmob srh print
#
impact bn=3.4e7 an=2.9e8
impact bn=3.4e7 an=2.9e8
```

```
#
contact  name=gate workfun=5.0
#
# SECTION 4: Id-Vd calculation
#
method gummel  newton itlim=20 trap  maxtrap=10 vsatmod.inc=0.01 carriers=2
output con.band val.band band.param e.mobility h.mobility
solve vgate=0
#
save outf=NPSGaNHemt0_0.str
tonyplot  NPSGaNHemt0_0.str
#
log outf=NPSGaNHemt0_0.log  master
#
method  newton trap itlim=35  maxtrap=6    carriers=2
solve vdrain=0.0  vstep=0.1  name=drain vfinal=1 vsource=0.0 vgate=0.0
solve vdrain=1.0  vstep=0.5  name=drain vfinal=5 vsource=0.0 vgate=0.0
solve vdrain=5.0  vstep=0.75  name=drain vfinal=20 vsource=0.0 vgate=0.0
#
save outf=NPSGaNHemt0_1.str
tonyplot  NPSGaNHemt0_0.log
#
quit
```

THIS PAGE INTENTIONALLY LEFT BLANK

APPENDIX B. ELECTRON CONCENTRATION GRAPHICS

1. 0 VOLT GATE BIAS

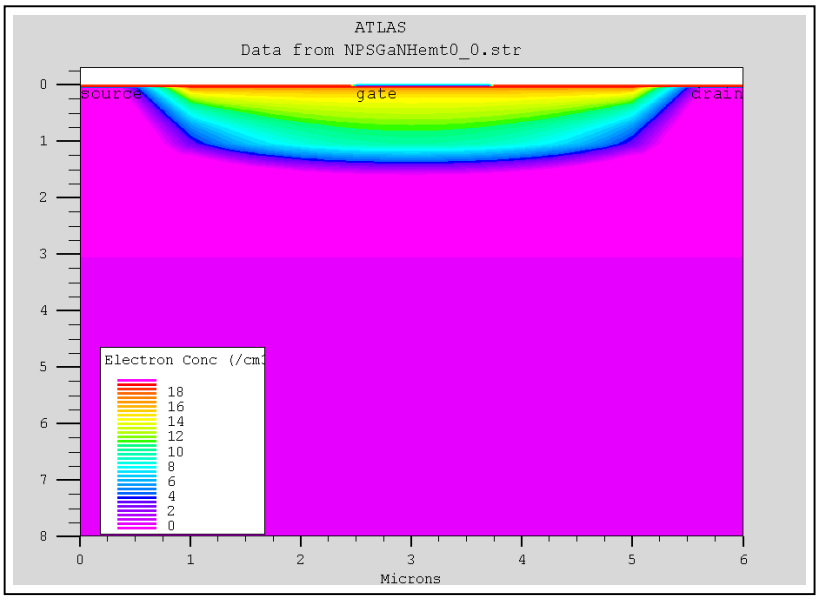

Figure B1. V_g =0 volts, V_d = 0 volts

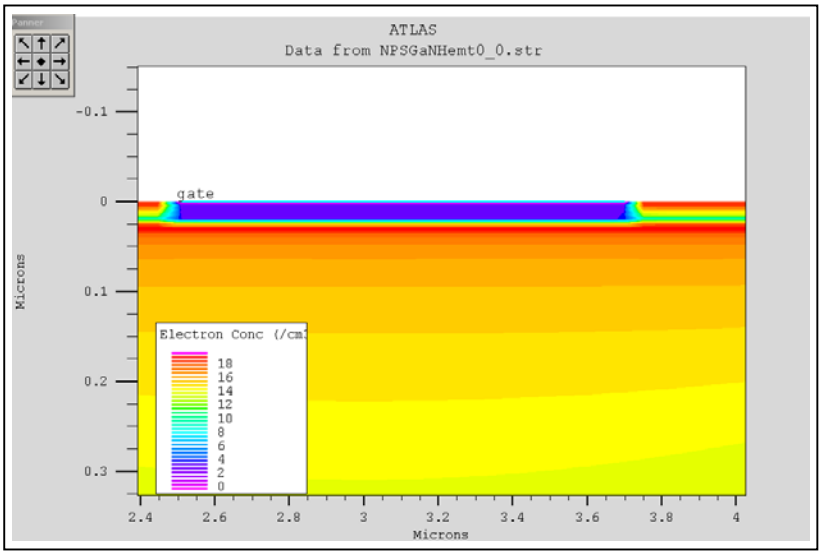

Figure B2. Close-up of V_g =0 volts, V_d = 0 volts

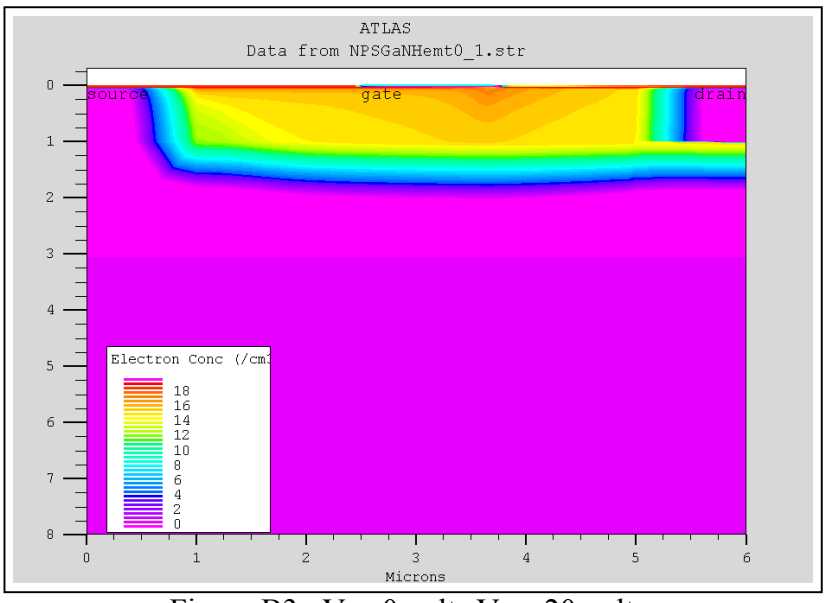

Figure B3. V_g =0 volts V_d = 20 volts

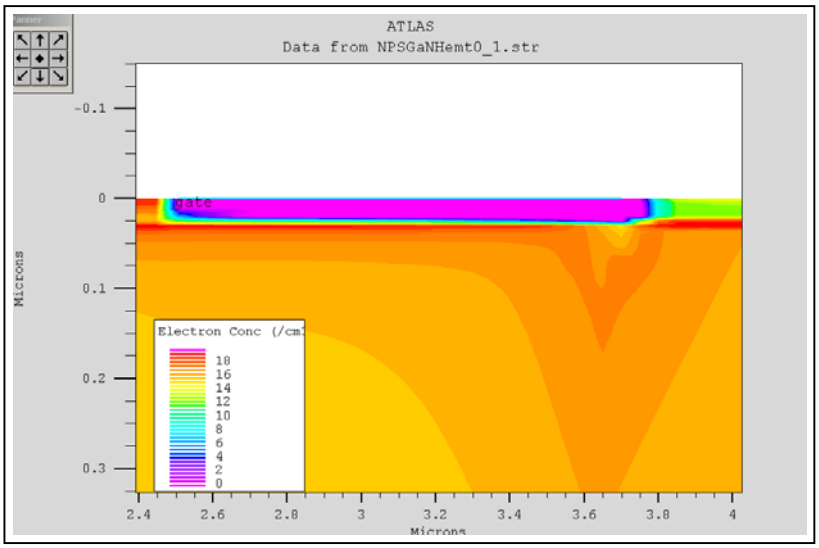

Figure B4. V_g =0 volts V_d = 20 volts

2. -1 VOLT GATE BIAS

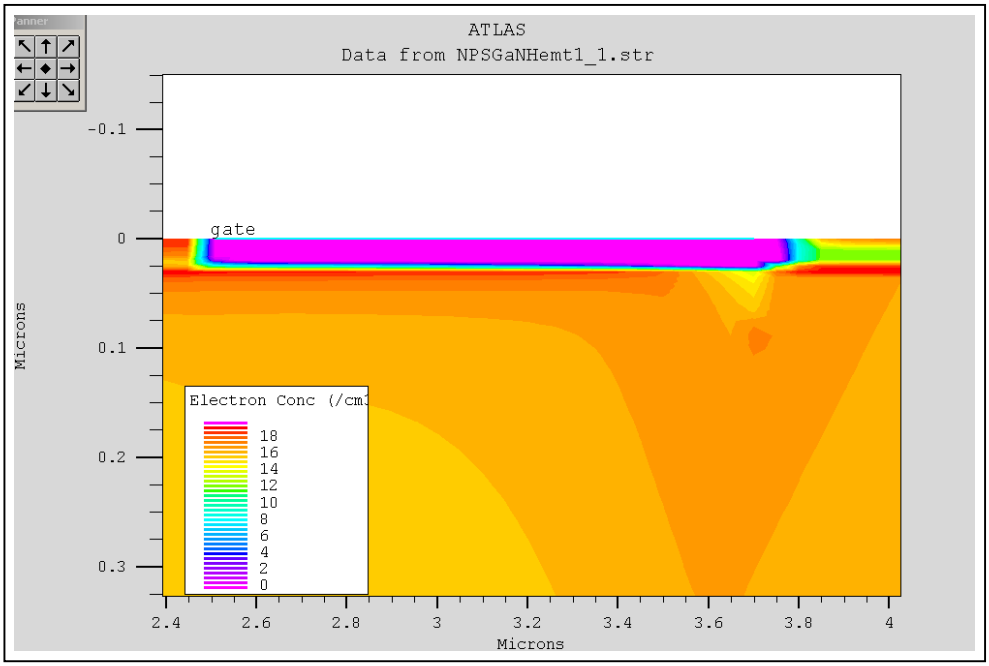

Figure B5. Close-up V_g = -1 volt, V_d = 20 volts

3. -2 VOLT GATE BIAS

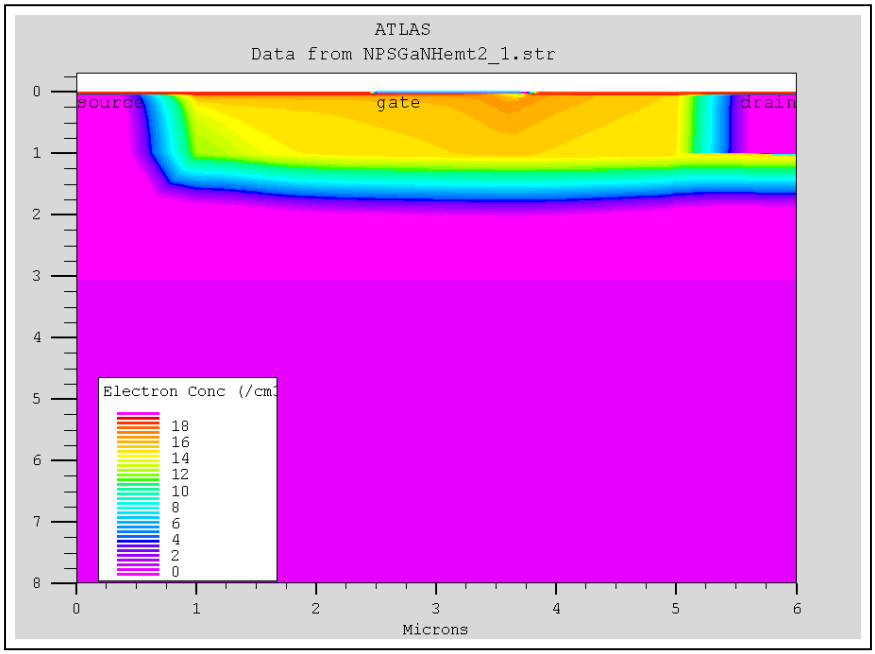

Figure B6. V_g = -2 volts, V_d = 20 volts

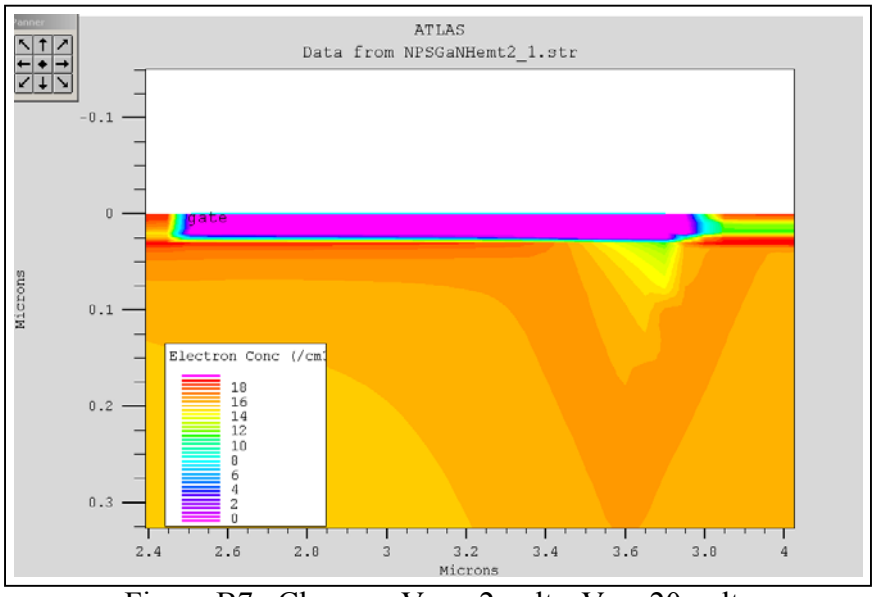

Figure B7. Close-up V_g = -2 volts, V_d = 20 volts

4. -3 VOLT GATE BIAS

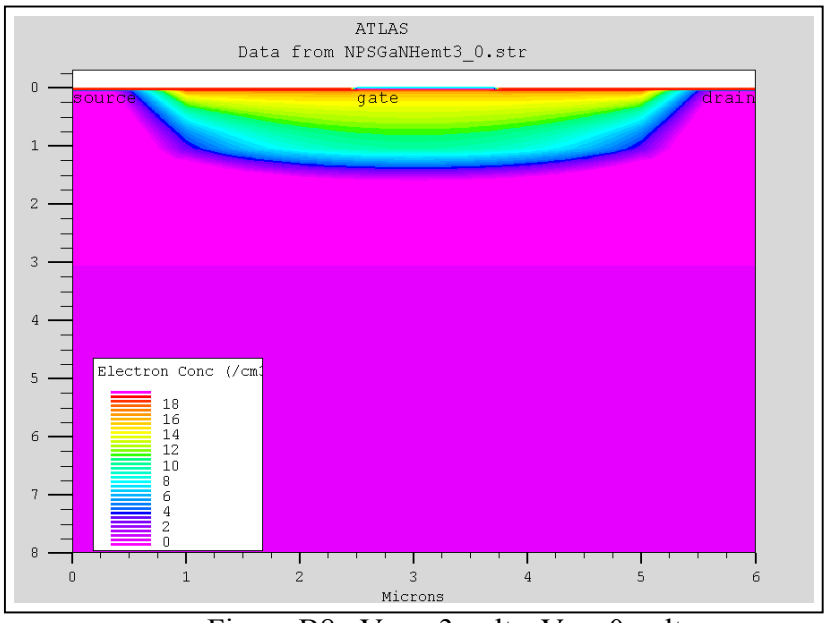

Figure B8. V_g = -3 volts, V_d = 0 volts

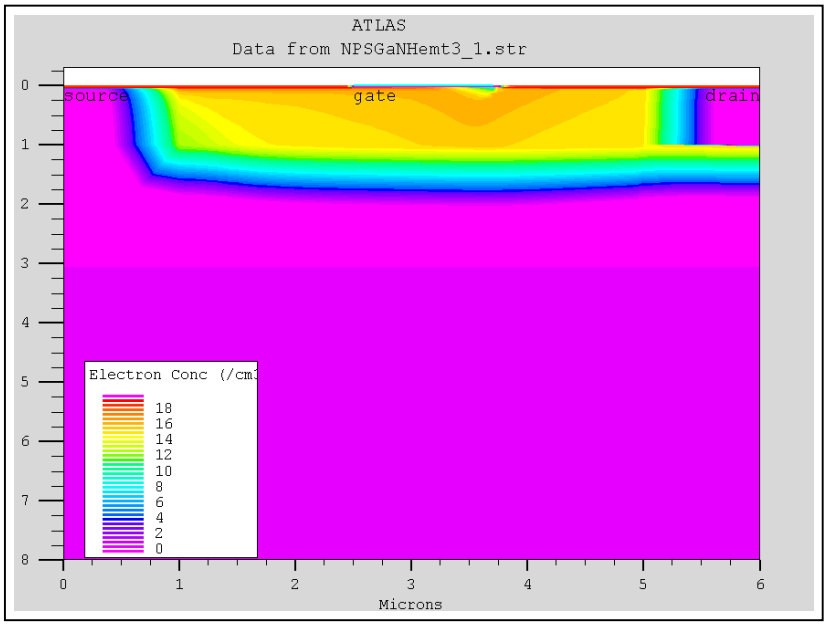

Figure B9. V_g = -3 volts, V_d = 20 volts

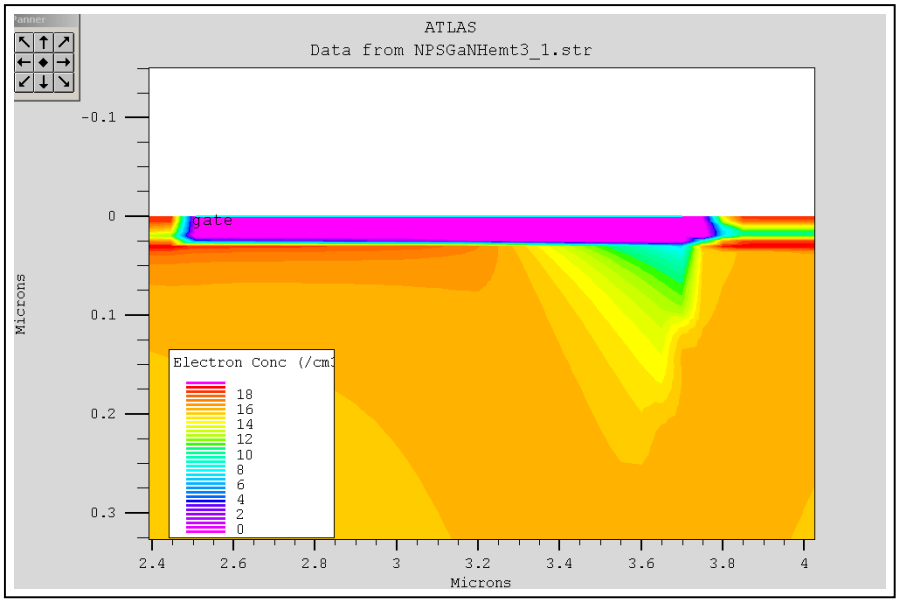

Figure B10. Close-up V_g = -3 volts, V_d = 20 volts

5. -4 VOLT GATE BIAS

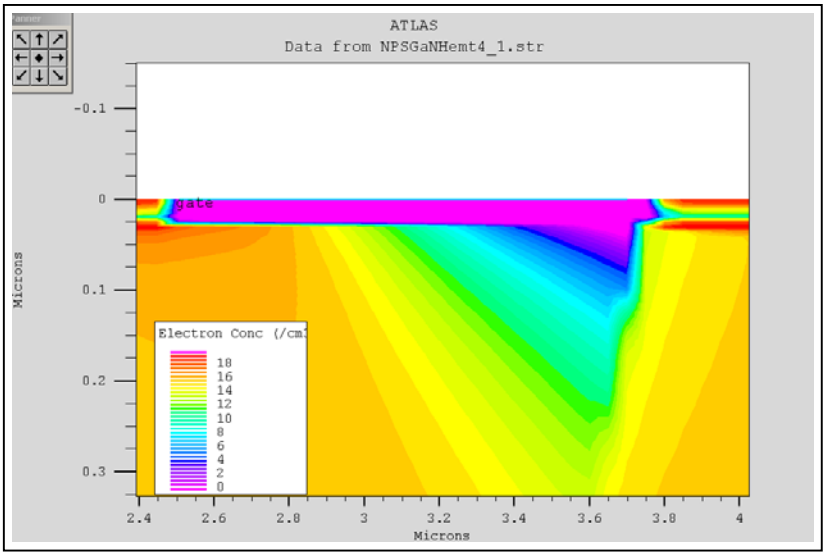

Figure B11. Close-up V_g = -4 volts, V_d = 20 volts

6. -5 VOLT GATE BIAS

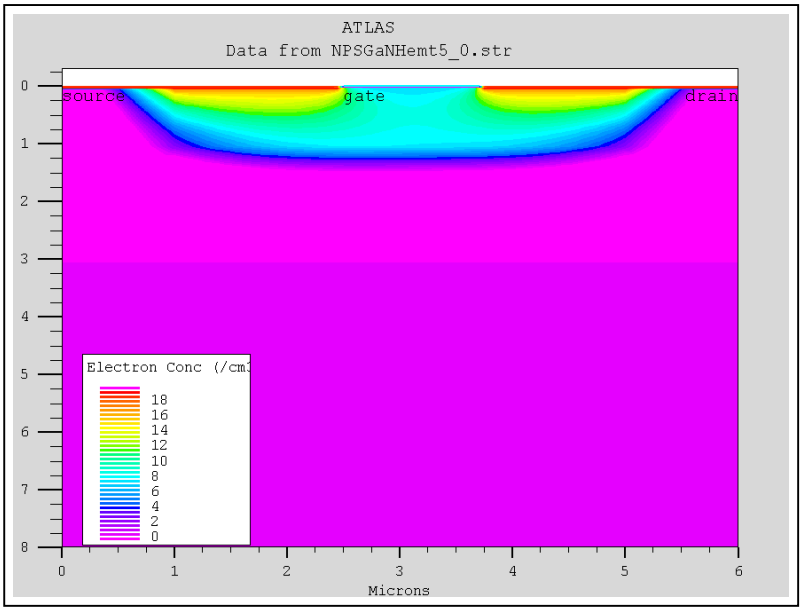

Figure B12. V_g = -5 volts, V_d = 0 volts

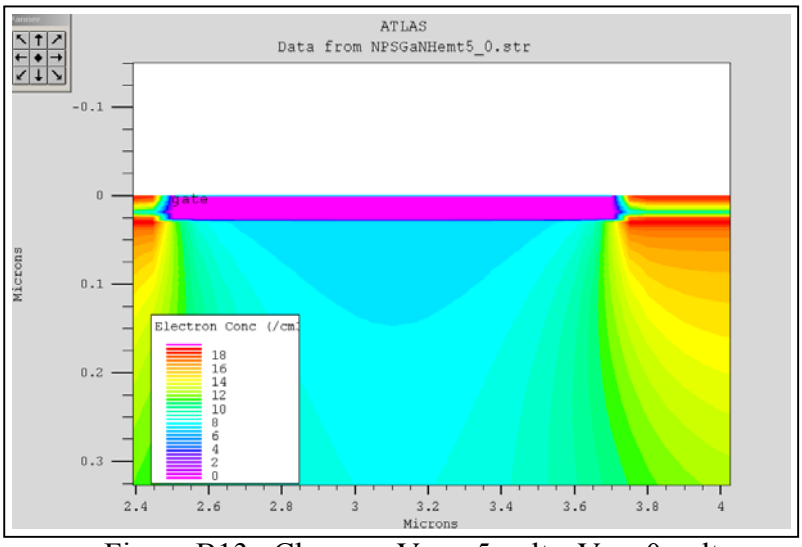

Figure B13. Close-up V_g = -5 volts, V_d = 0 volts

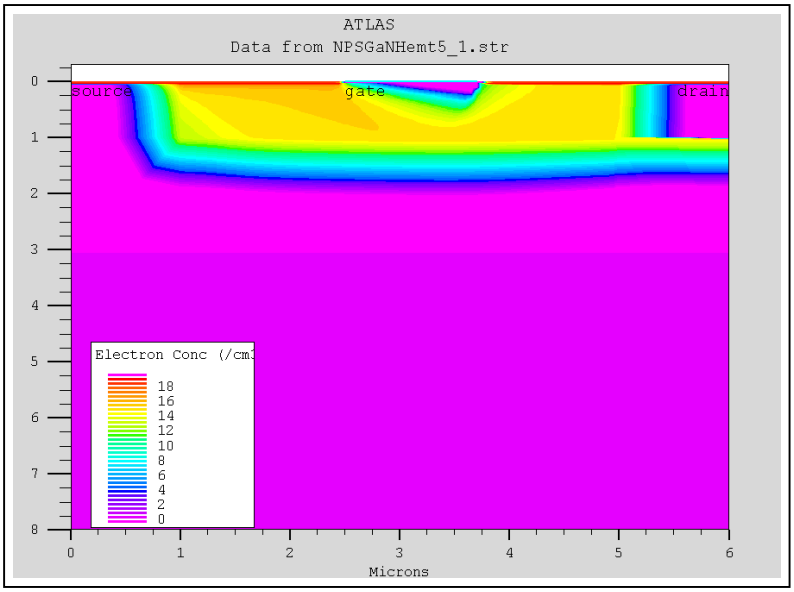

Figure B14. Close-up V_g = -5 volts, V_d = 20 volts

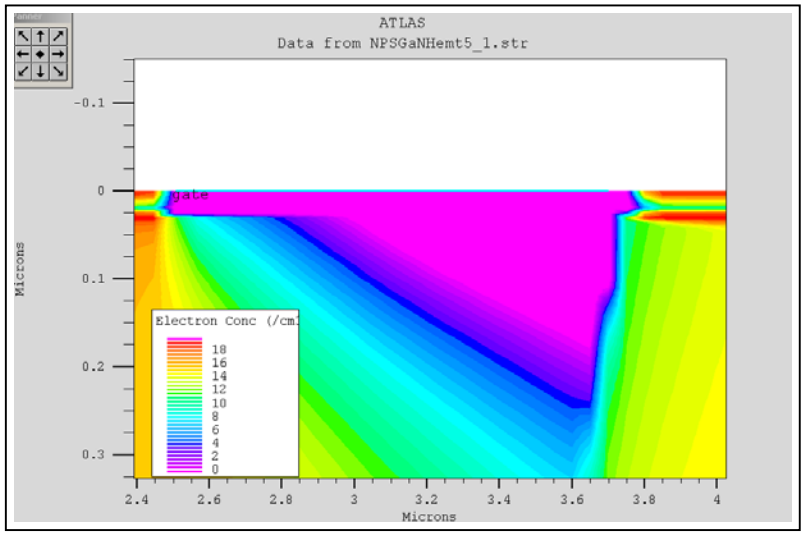

Figure B15. Close-up V_g = -5 volts, V_d = 20 volts

THIS PAGE INTENTIONALLY LEFT BLANK

APPENDIX C. TRANSCONDUCTANCE AND SUBTHRESHOLD

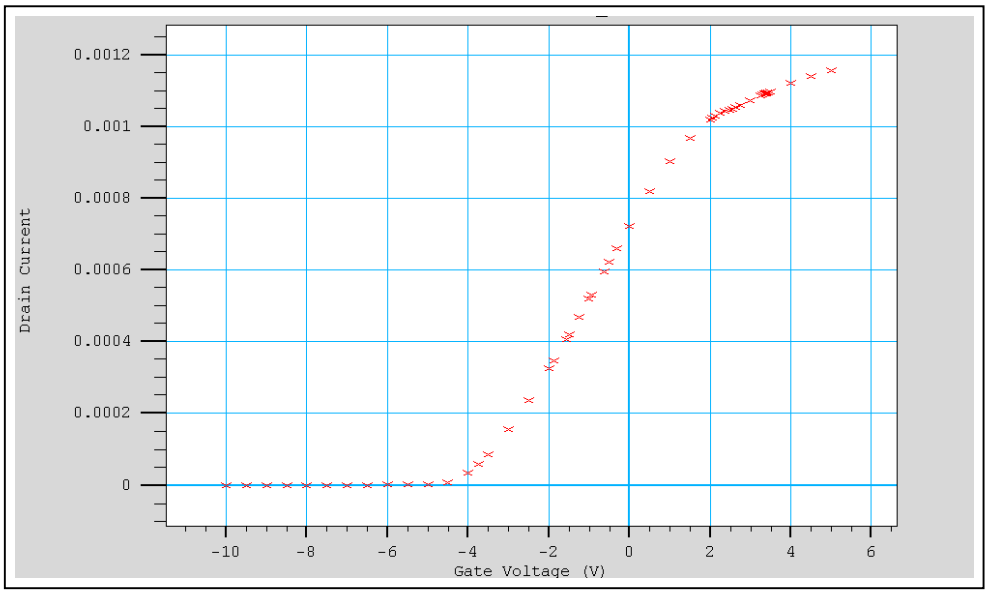

Figure C1. Transconductance Plot

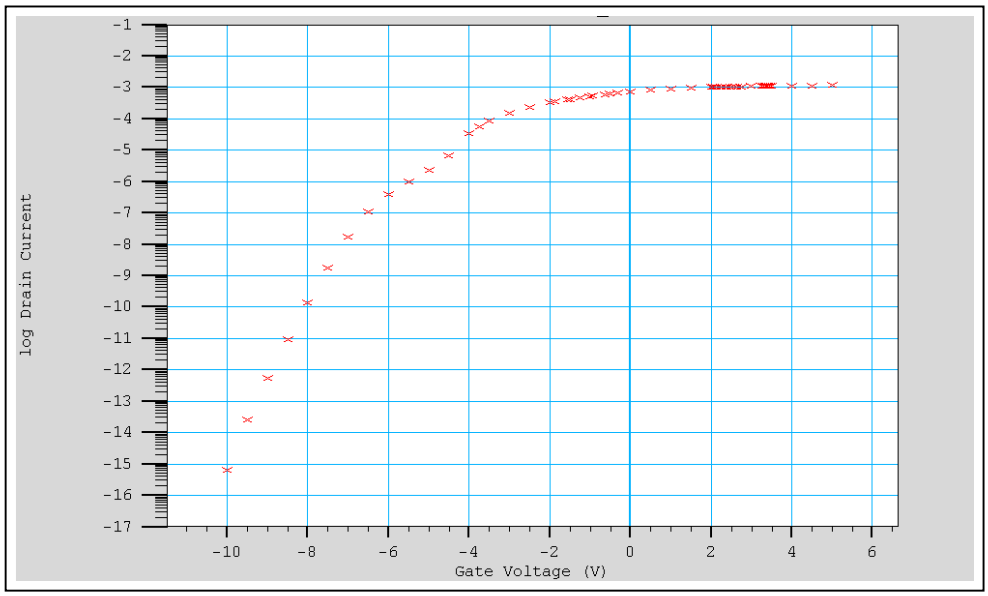

Figure C2. Subthreshold Plot

THIS PAGE INTENTIONALLY LEFT BLANK

APPENDIX D. DECKBUILD SIMULATION INPUT DECK

```
go atlas
Title    AlGaN/GaN HEMT with AlN Nucleation Layer
#        based upon NRL experimental HEMT (0.3 Al mole fraction)
#         Vg = 0V
#        Simulated separation of charges
#
#
# SECTION 1: Meshing Parameters
#
mesh

x.mesh loc=0.0  spac=1.0
x.mesh loc=1.0  spac=0.1
x.mesh loc=3.0  spac=0.05
x.mesh loc=5.0  spac=0.05
x.mesh loc=6.0  spac=1.5

y.mesh loc=0.0    spac=0.005
y.mesh loc=0.025  spac=0.005
y.mesh loc=1.0   spac=0.05
y.mesh loc=3.025  spac=2.0
y.mesh loc=3.055  spac=2.0
y.mesh loc=8.0    spac=3.0
#
#
# SECTION 2: Structure Specification
#
region     num=1  material=AlGaN y.min=0.0 y.max=0.025 x.composition=0.3
region     num=2  material=GaN y.min=0.025 y.max=3.025
```

```
region     num=3  material=AlN y.min=3.025 y.max=3.045
region     num=4  material=Sapphire y.min=3.045 y.max=8
#
elec       num=1  name=source x.min=0.0 x.max=0.0 y.min=0.0 y.max=1.0
elec       num=2  name=gate   x.min=2.5 x.max=3.7 y.min=-0.5 y.max=0.0
elec       num=3  name=drain  x.min=6.0 x.max=6.0 y.min=0.0 y.max=1.0
#
# Separate Charges
# Simulate Spontaneous Polarization
doping     uniform y.min=0.0 y.max=0.005 n.type conc=2.5e18
doping     uniform y.min=0.019 y.max=0.024 p.type conc=2.5e18
doping     uniform y.min=0.03 y.max=0.035 n.type conc=1.e19
doping     uniform y.min=3.000 y.max=3.024 p.type conc=1.e18

# Simulate Piezoelectric Polarization
doping     uniform y.min=0.0 y.max=0.005 n.type conc=2.5e18
doping     uniform y.min=0.019 y.max=0.024 p.type conc=2.5e18
doping     uniform y.min=0.03 y.max=0.035 n.type conc=1.e19
doping     uniform y.min=3.000 y.max=3.024 p.type conc=1.e18
#
#


#
# SECTION 3: Material Models
#
material material=AlGaN  mun=600 mup=10 affinity=3.82 nc300=2.07e18
material material=AlGaN nv300=1.16e19 eg300=3.96 align=0.8
permittivity=10.32
#
material material=GaN  mun=900 mup=10 nc300=1.07e18
material material=GaN  nv300=1.16e19 eg300=3.4 align=0.8
```

```
material material=GaN  arichn=24 arichp=96 edb=0.025 eab=0.160
material material=GaN  permittivity=9.5 vsatn=2e7
#
model material=AlGaN conmob fldmob srh print
model material=GaN conmob fldmob srh print
#
impact bn=3.4e7 an=2.9e8
impact bn=3.4e7 an=2.9e8
#
contact  name=gate workfun=5.0
#
# SECTION 4: Id-Vd calculation
#
method gummel  newton itlim=20 trap  maxtrap=10 vsatmod.inc=0.01 carriers=2
output con.band val.band band.param e.mobility h.mobility
solve vgate=0
#
save outf=NPSGaNHemt0_0.str
tonyplot  NPSGaNHemt0_0.str
#
log outf=NPSGaNHemt0_0.log  master
#
method  newton trap itlim=35  maxtrap=6    carriers=2
solve vdrain=0.0  vstep=0.1  name=drain vfinal=1 vsource=0.0 vgate=0.0
solve vdrain=1.0  vstep=0.5  name=drain vfinal=5 vsource=0.0 vgate=0.0
solve vdrain=5.0  vstep=0.75  name=drain vfinal=20 vsource=0.0 vgate=0.0
#
save outf=NPSGaNHemt0_1.str
tonyplot  NPSGaNHemt0_0.log
#
quit
```

THIS PAGE INTENTIONALLY LEFT BLANK

INITIAL DISTRIBUTION LIST

1. Defense Technical Information Center
   8725 John J. Kingman Road, Suite 0944
   Ft. Belvoir, VA 22060-6218

2. Dudley Knox Library
   Naval Postgraduate School
   411 Dyer Road
   Monterey, CA 93943-5101

3. Engineering and Technology Curricular Office, Code 34
   Naval Postgraduate School
   Monterey, CA 93943-5109

4. Chairman, Code EC
   Department of Electrical and Computer Engineering
   Naval Postgraduate School
   Monterey, CA 93943-5121

5. Prof. Todd R. Weatherford, Code EC/Wt
   Department of Electrical and Computer Engineering
   Naval Postgraduate School
   Monterey, CA 93943-5121

6. Prof. Ronald Pieper, Code EC/Pr
   Department of Electrical and Computer Engineering
   Naval Postgraduate School
   Monterey, CA 93943-5121

7. LT Kenneth L. Holmes, USN
   650 Barth Court
   Marina, CA 93933